Influence of pyro-gasification and activation conditions on the porosity of activated biochars: A literature review

Flavia Lega Braghiroli [1], Hassine Bouafif [1], Carmen Mihaela Neculita [2], Ahmed Koubaa [3]

[1] *Centre Technologique des Résidus Industriels* (Technology Center for Industrial Waste – CTRI), *Cégep de l'Abitibi-Témiscamingue* (Abitibi-Témiscamingue College), 425 Boul. du Collège Rouyn-Noranda, QC J9X 5E5, Canada

[2] *Research Institute on Mines and the Environment* (RIME), *Université du Québec en Abitibi-Témiscamingue* (University of Québec in Abitibi-Témiscamingue – UQAT), 445 Boul. de l'Université, Rouyn-Noranda, QC J9X 5E4, Canada

[3] *Institut de recherche sur les forêts* (Research Forest Institute – IRF), *Université du Québec en Abitibi-Témiscamingue* (University of Québec at Abiti-Témiscamingue – UQAT), 445 Boul. de l'Université, Rouyn-Noranda, Québec, QC J9X 5E4, Canada

[*] Corresponding author: (F.L. Braghiroli); Tel: +1 (819)-762-0931 ext. 1748; Fax: +1 (819)-762-0906; Email: Flavia.Braghiroli@uqat.ca

Abstract

Biochar is a carbon-rich organic material that has advantageous physicochemical properties for applications in multidisciplinary areas of science and engineering, including soil amendment, carbon sequestration, bioenergy production, and site rehabilitation. However, the typically low porosity and surface area of biochars (from 0.1 to 500 m^2 g^{-1}) limits the suitability for other applications, such as catalysis, electrochemistry, energy storage, and contaminant sorption in drinking water and wastewater. Given the high global demand for activated carbon products, scientists and industrialists are exploring the potential of biochar-derived biomass as precursors for activated carbons. This review presents and discusses the available studies on activated biochars produced from various precursor feedstocks and under different operating conditions in a two-step procedure: pyro-gasification (torrefaction, slow to flash pyrolysis, and gasification) followed by activation (physical, chemical or physicochemical). Findings from several case studies demonstrate that lignocellulosic residues provide attractive precursors, and that chemical activation of the derived biochars at high temperature and long residence time produces highly porous end materials. Indeed, the porosity of activated biochars varies greatly (from 200 to 2500 m^2 g^{-1}), depending on the pyro-gasification operating conditions and the feedstock (different feedstocks have distinct morphological and chemical structures). The results also indicate that the development of highly porous activated biochars for diverse purposes (e.g., electrodes for electrochemical energy storage devices, catalyst supports and adsorbents for water treatment) would benefit both the bioeconomy and the environment. Notably, it would leverage the potential of added-value biomass as an economical, non-fossil, readily available, and renewable energy source.

Keywords: Biomass residue waste, pyro-gasification, biochar, activation, porous carbon materials

Graphical abstract:

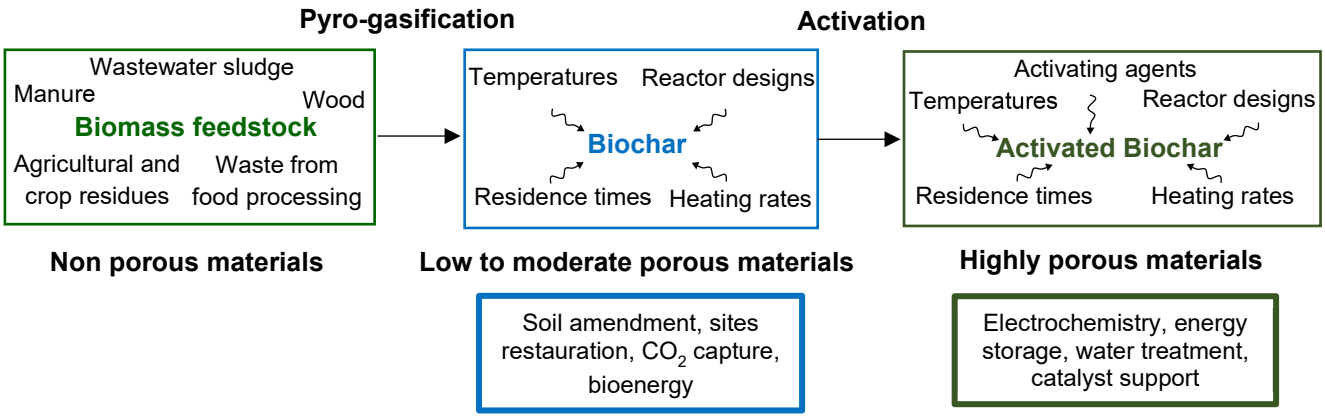

Statement of novelty:

Variations in biomass feedstock and pyro-gasification operating conditions can strongly influence the porosity of activated biochars to be applied in a variety of fields, including environmental protection and energy storage. The production of activated biochars would provide multiple benefits, both economic and environmental. Economically, biorefineries could diversify their product offer (biochar, bio-oil, and syngas) to include activated biochars. Environmentally, biomass provides a cost-effective, renewable, and eco-friendly fuel source.

Terms and definitions:

Char: A solid material generated by incomplete combustion processes that occur in natural and man-made fires [1].

Charcoal: A solid material produced by thermochemical conversion of biomass and used for energy generation [2].

Coal: Organic sedimentary rock consisting of a complex mixture of organic and mineral substances derived from ancient plant deposits [1].

Peat: A naturally occurring material formed by the biodegradation of organic substances derived from ancient plant deposits under limited oxygen conditions [1].

Coke: A solid material produced by heating coal in the absence of air [3].

Biochar: A solid material obtained from the thermochemical conversion of biomass in a zero or low oxygen environment [2].

Hydrochar or HTC material: A solid product obtained from hydrothermal carbonization (HTC).

Activated carbon: A material derived from either a natural (hardwood, coconut shells, fruit stones, coal) or synthetic macromolecular compounds that has undergone activation. Activation is the selective gasification of carbon atoms using steam, CO_2, or chemicals at increasing temperature [1].

Activated biochar: A biochar that has undergone activation.

* Corresponding author: (F.L. Braghiroli); Tel: +1 (819)-762-0931 ext. 1748; Fax: +1 (819)-762-0906; Email: Flavia.Braghiroli@uqat.ca

1. Introduction

Recent studies and reviews have advanced the knowledge on biochar structure and characteristics along with its potential uses in agriculture and industrial applications. Biochars prepared with different thermochemical processes and under different operating conditions can be characterized by the physicochemical properties (e.g., carbon content, surface area and porosity, cation exchange capacity, water holding capacity) that are desirable for various end uses. In addition, biochar contains noncarbonized materials and several functional groups such as O-containing carboxyl, hydroxyl, and phenolic molecules, all of which can bind to and interact with contaminants and organic matter. Fig. 1 summarizes the main products (gas, liquid, and solid) obtained from thermochemically modified biomass residues using different reactor designs, temperatures, residence times, and heating rates in an inert system, along with the main end uses. Among others, the end products are used to generate bioenergy (manufactured biochar pellets) [4, 5], restore degraded sites (e.g., abandoned mine sites) [6, 7], and amend agricultural soil [8, 9].

Given the high global demand for activated carbon products, which is projected to post $4.9 billion in revenues by 2021 [10], scientists and industrialists are exploring the potential of biochar-derived biomass as precursors for activated carbons. Therefore, to improve the porous structure and expand the adsorptive capacity of biochars, activation is applied as a second step. The activation conditions are more intense: higher temperature (e.g., 1173 K), the presence of chemicals and/or gases (e.g., KOH, H_3PO_4, CO_2, steam), and longer residence times (e.g., 1−2 h) in an inert atmosphere. At such conditions, the low surface area and high volatile matter content of the biochars, which result from the reactor conditions during biochar preparation: low pyro-gasification temperature (e.g., 593 K), short residence time (e.g., 1–2 s), and rapid heating rate (e.g., faster than

300 K min^{-1}), will be improved. Therefore, to expand the range of applications, the biochars are activated to produce highly porous and effective materials for use in electrolytic capacitors [11, 12], batteries [13], and electrochemical energy storage devices [14, 15]; as catalyst supports [16, 17]; and as precursors for adsorbent production [18, 19].

This review is structured into two parts. First, the biochar production processes and material properties are outlined, including thermochemical conversion methods and the various types of biomass feedstocks. The mechanisms involved in biochar transformation are then described, along with the gas analysis methods currently used to determine the porosity of biochars. The factors that affect biochar characteristics, particularly surface and textural properties, are also explained. Second, the activation processes that improve surface porosity and optimize functionality are presented. The most commonly used methods are described, and the research on activated biochars and the factors that affect their porous structure is reviewed. The Supplementary Material (Table 1S) presents a compilation of publications on activated biochars derived from different feedstocks (crop residues, wood biomass, animal litter, sewage sludge, solid waste) and using various pyro-gasification and activation operating conditions. The main reactor designs for producing activated biochars available in the open literature are then summarized, the challenges are appraised, and future research avenues are proposed.

2. Biochar production and properties

2.1. Biomass thermoconversion

Depending on the feedstock source, seven main thermal conversion processes are used to produce biochar as a main product or by-product: gasification; flash, fast, intermediate, and slow pyrolysis; torrefaction; and hydrothermal carbonization. According to the reactor design and its operational parameters, the final materials contain various proportions of the relative quantity and

quality of liquid (bio-oil), solid (hydrochar, torrefied biomass, or biochar), and gas (syngas, composed mainly of CO and H_2). Table 1 summarizes the most important characteristics of the pyro-gasification processes, the main products, and the solid yield (adopted from Ahmad et al. [20], Bolan et al. [21], Bridgwater [22], Brown [23], and Laird et al. [24]). Gasification, which converts most of the biomass into gas at temperatures higher than 1073 K and residence times of 10–20 s, obtains a low percentage of biochar (around 10 wt.%). Flash pyrolysis yields slightly more biochar (10–20 wt.%) at temperatures of 673−1273 K and very high heating rate (~ 1000 K min^{-1}), with syngas as the main product. Fast pyrolysis, at temperatures of 573−1273 K and with very short residence time (< 2 s), yields about 12 wt.% biochar. Intermediate pyrolysis, at approximately 773 K with residence times of 10–20 s, produces about 25 wt.% biochar, whereas slow pyrolysis, at temperatures of 373−1273 K and residence times of 5−30 min, yields about 35 wt.% biochar. Torrefaction requires temperatures of 473−593 K, and it obtains almost 80 wt.% of torrefied biomass. Finally, hydrothermal carbonization is a wet thermochemical process that uses a hot (453−533 K) and pressurized (1−4.7 MPa) water environment to convert biomass (or wet biomass, e.g., wastewater sludge) into fuels such as hydrochar and liquid fuels [25].

Biomass can be converted at low cost either by applying thermochemical processes to agricultural residues on site or by integrating thermochemical processes into existing industrial operations related to biomass residue waste. Thus, biomass waste from both agricultural and industrial operations can be turned into valuable by-products, thereby lowering waste transport and storage costs. For example, Zabaniotou et al. [26] demonstrated the economic, environmental, and social benefits of a small-scale biomass pyrolysis system at an olive farm in the Mediterranean region. The results showed that 70 t of solid waste from 10 ha of olive groves and the milling process were converted into 13, 11, and 12 t of liquid, biochar, and gas fuel, respectively. The fuel

169 by-product met the olive milling energy needs, and biochar was applied to improve the
170 physicochemical and microbiological fertility of the soil. Farmers and small communities could
171 install similar pyrolysis units to produce heating fuel and biochar for soil amendment.

172 **2.2. Mechanisms of biochar production**

173 Biochar is a product formed from two solid-phase reactions. The primary reactions are highly
174 endothermic [27], and the resultant char has an aromatic polycyclic structure [28]. As the biomass
175 converts into a carbonaceous residue (i.e., the primary biochar), organic vapors (tars) decompose
176 to form coke [29]. The primary vapor-phase reaction products, which are unstable, then undergo
177 secondary exothermic reactions: cracking and repolymerization. The primary and secondary
178 reactions occur differently, depending on the type of thermochemical conversion (e.g., slow or fast
179 pyrolysis). With its long residence time, slow pyrolysis maximizes the char yield. Consequently,
180 both the primary and secondary reactions are involved in biochar formation [30]. In contrast, fast
181 pyrolysis maximizes the condensable vapor yield (bio-oil) due to the higher heating rate and short
182 holding time of volatiles that interrupts the occurrence of secondary reactions [31, 32].

183 Most biomass residues are lignocellulosic, meaning that they contain the fibrous part of plant
184 materials that consists mainly of cellulose, hemicellulose, lignin, extractives, and ash (including
185 inorganics) [33]. During lignocellulosic biomass pyro-gasification, the first three of these
186 components are thermally modified by means of different mechanisms and paths. Cellulose
187 decomposes at temperatures of 513−623 K [34, 35], hemicellulose at temperatures of 473−533 K,
188 and lignin within the highest (and widest) temperature range of 553−773 K [36–38]. The most
189 complex of these is lignin decomposition, and the precise mechanism remains challenging to
190 understand and depict. What is known is that free radicals are generated when β-O-4 lignin bonds
191 are cleaved [39, 40]. These free radicals capture protons from other species with weak C–H or O–

192 H bonds to form bio-oil compounds such as vanillin and 2-methoxy-4-methylphenol [39, 41]. They
193 also react with other species, leading to chain extension, and they collide with each other to form
194 solid stable compounds, such as biochar [42].

195 Cellulose initially depolymerizes into oligosaccharides, followed by cleavage of the glycosidic
196 bond to produce D-glucopyranose. Then, through certain intramolecular rearrangements,
197 levoglucosan (1,6-anydro-β-D-glucopyranose) is formed [43]. Levoglucosan is a major constituent
198 of the condensable fraction (bio-oil) [44]. Furthermore, it acts as an intermediate material during
199 cellulose decomposition, which can take one of two paths: 1) levoglucosenone can form through
200 dehydration, followed by decarboxylation, aromatization, and intramolecular condensation, to form
201 solid biochar; or 2) levoglucosan can undergo a series of rearrangement and dehydration processes
202 to form hydroxymethylfurfural, which may then decompose to produce bio-oil and syngas, and/or
203 it can polymerize into biochar by means of aromatization and intramolecular condensation reactions
204 [45–49].

205 The hemicellulose decomposition mechanism is relatively similar to that for cellulose. First,
206 hemicellulose depolymerizes to form oligosaccharides, followed by cleavage of the glycosidic
207 bonds in the xylan chain. The rearranged depolymerized molecules then form 1,4-Anhydro-D-
208 xylopyranose, an intermediate product in hemicellulose decomposition by pyro-gasification, which
209 follows two main alternative paths: 1) several reactions such as dehydration, decarboxylation,
210 aromatization, and intramolecular condensation, resulting in the formation of solid biochar; or 2)
211 decomposition, which produces low molecular weight bio-oil and syngas compounds [50–52].

212 Mineral nutrients (e.g., K^+, Na^+, Ca^{2+}, Mg^{2+}, Cl^-, NO^{3-}, OH^-, CO_3^{2-}, PO_4^{3-}) that are present in
213 biomass feedstock can also catalyze thermolysis reactions and alter the chemical composition of
214 the resultant solid material [37]. Because the primary reaction products form via competitive

215 reactions, these minerals can have different effects. For example, they influence the formation of
216 low molecular weight species (e.g., formic acid, glycolaldehyde, and acetol), furan ring derivatives
217 (e.g., 2-furaldehyde and 5-hydroxy methyl furfural), and levoglucosan. In an experiment using
218 varying concentrations of inorganic salts impregnated on pure cellulose, faster competing reactions
219 lowered the levoglucosan yield depending on the cation or anion type, due to the formation of low
220 molecular weight species from the cellulose [53], and this may have interfered with the formation
221 mechanism, yield, and composition of the resultant biochars.

222 Other kinds of biomass feedstock are thermally modified by different pathways due to their
223 complex chemical structure, compared to lignocellulosic materials. For example, algae species
224 contain proteins, carbohydrates, lipids, nitrogen and ashes. Then, a multi-step mechanism of the
225 thermal decomposition of such components have been proposed in the available literature [54].
226 According to Debiagi et al. [54], the thermal degradation of macroalgae starts with the
227 decomposition of 1) carbohydrates and lipids, then 2) protein components (~ 573 K), and 3)
228 metal carbonates and salts (> 973 K). In the first steps, sugars and triglycerides are degraded,
229 whereas low molecular weight proteins are depolymerized into nitrogen tar components: pyrrole,
230 pyridine, and diketopiperazine together with gas species. The release of ammonium, nitrates and
231 carbonates groups can be also estimated according to the ash content.

232 The herbaceous biomass contains typically important amounts of mineral inorganic compounds
233 (4–16 %), which have significant influence on the decomposition of lignocellulosic compounds
234 mechanisms, as mentioned earlier [34]. Another group of biomass with a complex chemical
235 composition is the sewage sludge coming from wastewater treatment systems. It normally contains
236 around 30 % of carbon and very high percentage of mineral inorganics (up to 60 %) [55]. Very few
237 studies focused on the mechanisms of the formation of pyro-gasification products due to the

complex reactions among organic matter, dead bacteria and non-biodegradable fractions [56]. The volatile matter and ash content present in sewage sludge had a significant influence on pyro-gasification products characteristics and distribution according to Fonts et al. [55]. Fullana et al. [57] also mentioned that a variety of nitrogenated compounds (nitriles, pyridines, amides, amines and polyaromatic nitrogenated) may also play a role on the final products quality. Finally, animal bones, another precursor used for the production of activated biochar, normally contains only 11 % of carbon and up to 78 % of calcium phosphate [58]. No mechanisms were found on the solid formation but the solid material obtained after pyrolysis contained about 70–76 % calcium hydroxyapatite ($Ca_{10}(PO_4)_6(OH)_2$), 9–11 % carbon, 7–9 % $CaCO_3$, 0.1–0.2 % $CaSO_4$ and 0.3 % Fe_2O_3 according to Iriarte-Velasco et al. [59].

2.3. Porosity of biochars

Several methods are used to analyze and assess the material structure of biochars and activated biochars. However, in this work, the focus is put on gas adsorption techniques to characterize the porosity of biochars and also activated biochars. When less organized bound carbonaceous material is removed during thermal treatment, the spaces that remain between the crystallites in biochar and activated biochar represent the material's porosity. The surface area of the solid material, which generally increases with increased pyro-gasification temperature, is used to indicate the adsorption capacity [1, 60–62]. The adsorption of Kr, N_2, or CO_2 is used to determine the surface area (S_{BET}) and textural structure of the porous material. Kr is used to analyze biomass materials, which have very low surface area, due to the lower vapor pressure (267 Pa) required compared to N_2 (101325 Pa) at 77 K [63]. The lower the saturation vapor pressure at the adsorption measurement temperature, the more accurate the measurement of low surface areas. In comparison, for highly microporous biochar materials, CO_2 adsorption can provide a more accurate measure of

261 ultramicropore volume, as it is used at higher temperatures (e.g., 273 K) compared to N_2 (e.g., 77
262 K). This is because N_2 can condense within the micropores and consequently block gas sorption.
263 For highly porous activated biochars, micro- and mesopore contents can be analyzed in terms of N_2
264 adsorption-desorption isotherms.

265 Several studies have assessed the influence of pyro-gasification temperature on the textural
266 properties of biochars. Chen and Chen [64] examined biochars derived from orange peels at
267 different pyrolytic temperatures (423–973 K) for 6 h. At the highest temperature (973 K), the
268 biochar presented the largest surface area, at 201 m^2 g^{-1} (0.035 cm^3 g^{-1}) compared to 23 m^2 g^{-1} (0.023
269 cm^3 g^{-1}) at 423 K. Graber et al. [65], Gray et al. [66], and Rehrah et al. [67] observed similar trends
270 using eucalyptus wood, hazelnut shells and Douglas fir chips, and pecan shells and switchgrass,
271 respectively, as feedstock. Generally, it has been suggested that biochars made from lignocellulosic
272 precursors have higher surface area due to the destruction of aliphatic alkyl and ester groups and
273 the breakdown of the lignin chain at higher pyro-gasification temperatures [64].

274 However, pyrolysis of pine wood produced very low surface area (29 m^2 g^{-1}) under specific
275 working conditions (973 K for 2 h) [68]. The difference in porosity between eucalyptus wood [65]
276 and pine wood [68] is attributable to the distinct molecular structures of the two taxonomic groups
277 to which they belong: hardwood (needle-leaved evergreen trees, angiosperms, or flowering plants)
278 and softwood (broadleaf deciduous trees, or gymnosperms), respectively. In the primary pyrolysis
279 stage, hardwood pyrolysis yields smaller amounts of char, which is more reactive for
280 devolatilization in the secondary reaction stage compared to softwood [69]. In addition, the
281 differences in thermochemical conversion between hardwood and softwood can be attributed to
282 three aspects: chemical components, molecular structure, and component proportion. The main
283 macromolecules in hardwood hemicellulose and lignin are acetylglucuronoxylan and syringyl,

284 respectively, whereas in softwood, the main macromolecules are galactoglucomannan,
285 glucomannan, and arabinoglucuronoxylan (in hemicellulose) and guaiacyl (in lignin) [70, 71]. The
286 proportions of cellulose, hemicellulose, and lignin also vary between hardwood and softwood:
287 hardwood contains lower hemicellulose and lignin (20–25 wt.% for both components) compared to
288 softwoods (25−30 wt.% for hemicellulose; 27−30 wt.% for lignin) [72]. The presence of extractives
289 composed of low molecular weight organic compounds (e.g., lipids, phenolic compounds,
290 terpenoids, fatty acids, resin acids, waxes) can also affect the thermal behavior of hardwood and
291 softwood in the low-temperature range [73].

292 Biochars produced from animal litter feedstock at higher pyrolysis temperatures also show
293 lower surface area compared to biochars produced from lignocellulosic residues. The materials in
294 animal litter are considered nongraphitizing carbons, due to either high oxygen or low hydrogen
295 contents. They are structured as individual, randomly orientated graphitic units with extensive cross
296 linking. In contrast, graphitizing carbons (such as lignocellulosic residues) are composed of parallel
297 graphitic units with a small number of cross linked units [74]. Other types of biochars produced
298 from rice husks and rice straw at 1073 K presented lower surface area: 296 and 257 m^2 g^{-1},
299 respectively, compared to biochar made from oak wood and apple wood chips (398 and 545 m^2 g^{-}
300 ^{1}, respectively) [61]. The properties of rice-derived biochar differed from those for wood-derived
301 biochar due to the high ash content (presence of inorganic components, particularly silicium). To
302 leverage these properties, the researchers proposed that combining inorganic compounds with
303 organic moieties could produce silicon-encapsulated carbon (the "silicon-and-carbon-coupled
304 framework model"), which could protect the biochar against physical and chemical oxidation and
305 provide potential stable carbon sequestration in soils [75].

306 Biochars are tailored for specific applications by taking advantage of the material's intrinsic
307 properties, including the cation exchange capacity (CEC), carbon sequestration potential, total and
308 fixed carbon contents, volatile matter content, chemical and physical recalcitrance (i.e., resistance
309 to biodegradation), surface area, pore volume, and average pore diameter. Several biomass
310 feedstocks, including cow and pig manure, waste wood, food waste, crop residues, aquatic plants,
311 and wastewater sludge, were submitted to slow pyrolysis at 773 K in N_2 atmosphere for 4 h at 18
312 K min^{-1} heating rate [76]. The total carbon content varied from 24.2 wt.% for bone dregs as
313 precursor to 75.8 wt.% for sawdust. The ash yield varied from 7.2 wt.% for wheat straw to 77.6
314 wt.% for bone dregs and the CEC varied from 23.6 cmol kg^{-1} for pig manure to 562 cmol kg^{-1} for
315 chlorella. Surface area and pore volume also varied considerably across precursors. When biochars
316 were prepared in the same pyrolysis conditions, surface area and total pore volume varied from
317 approximately 3 m^2 g^{-1} (0.01 cm^3 g^{-1}) for alga chlorella to 203 m^2 g^{-1} (0.13 cm^3 g^{-1}) for sawdust.
318 This heterogeneity of the composition, physicochemical properties, and structural characteristics of
319 biochars derived from different feedstocks underscores the difficulty of targeting specific soil or
320 environmental end uses. Nevertheless, biochar functionalization (e.g., activation) can be applied to
321 expand the range of adsorptive applications that require very high porosity (S_{BET} > 1000 m^2 g^{-1}).

322 **3. Biochar functionalization**

323 Recent advances in biochar functionalization, including surface tuning and porosity tailoring,
324 have provided new materials for the carbon chemistry field and innovative applications for several
325 other fields such as catalysis, energy storage, and pollutant removal. Structurally, biochars may
326 present either highly oxygenated groups (e.g., C−O, C=O, −OH) at the surface or else an oxygen-poor
327 surface, with few oxygenated or heteroatom groups. The biochar texture and surface chemistry are
328 responsible for a variety of physicochemical and catalytic properties [77, 78]. In carbonaceous

329 materials, the surface functionalities can be modified by directly incorporating heteroatoms during
330 biochar pre- or post-synthesis, via a number of methods: 1) surface oxidation, or exposure to
331 hydrogen peroxide, ozone, permanganate, or nitric acid to create oxygenated functional groups at
332 the surface [79]; 2) surface amination, or exposure to amino groups such as NH_3 [80–82]; and 3)
333 surface sulfonation, or exposure to sulfonic groups (SO_3H) [83, 84]. Another approach takes
334 advantage of the chemical composition of certain feedstock precursors that have high nitrogen
335 content (e.g., algae) or inorganic matter content (e.g., sewage sludge). In both cases, thermal
336 treatment produces functional groups in the carbonaceous structure and/or at the carbonaceous
337 surface [85, 55, 86]. This approach produces biochars with porosity and structural development as
338 well as catalytic active sites that enable catalytic reactivity, making them well suited for
339 contaminant adsorption [87].

340 Surface doping with metals is another way to functionalize biochar materials for specific
341 applications: metals (Fe, Zn, Ni, and Cu) are added to the biomass structure before or after thermal
342 treatment. In the case of Ni, adding the metal before can produce catalytic effects during the
343 pyrolysis reaction that will improve the biochar structure and enhance H_2 gas production [88].
344 Several studies have obtained promising results by adding high valent metals to biomass precursors,
345 thereby reducing the metals to zero valent metal nanoparticles [89–91] or metal oxide nanoparticles
346 [92–94]. Metal nanostructures have presented enhanced electronic, magnetic, optical, and chemical
347 properties over existing bulk materials [95–98].

348 Heavy metals can also be impregnated on the biochar surface to produce materials that adsorb
349 metalloids in contaminated waters. The metalloids are removed via complex formation or chelating
350 at the surface of the carbonaceous material [99, 100]. It was suggested that the ability to adsorb
351 heavy metals is due to electrostatic interactions between the biochar's negative surface charge and

352 metal cations as well as ion exchanges between the surface protons and metal cations [101, 102].
353 This allows removing certain metalloids (e.g., arsenic) that are typically present in minerals and
354 mine wastewater, and which mining industries in several countries are required to monitor. Hence,
355 impregnating biochar with transition metal ions or oxides (e.g., Cu, Fe, Zn) improved the sorbent
356 performance for more effective contaminant removal [103, 104].

357 To summarize, many effective functionalization methods have been developed to enhance the
358 performance of biochars, and particularly for catalysis and mining wastewater treatment. To tailor
359 the biochar pore structure for other adsorptive applications (e.g., electrochemistry, gas adsorption,
360 drinking water treatment), activation is the most commonly used procedure. The following sections
361 describe how biochars are activated as well as the optimal conditions (activation type, pyro-
362 gasification and activation operations) for improving porosity and expanding the range of potential
363 applications.

364 **4. Activation**

365 Activated carbons are widely used to treat effluents and industrial wastes, purify water, and
366 remove odors from gases [1, 105, 106]. This is due to the well developed porous structure, which
367 is obtained by high-temperature thermal treatment in the presence of activating agents. Specifically,
368 activation causes channels to form throughout the graphitic regions, spaces, and fissures within and
369 between the crystallites in the carbon, obtaining a large internal surface area [1, 107]. The final
370 porosity can be quantified and classified as microporosity (lower than 2 nm), mesoporosity (2 to 50
371 nm), and albeit rarely seen in activated carbons, macroporosity (higher than 50 nm).
372 Ultramicroporosity (less than 0.7 nm) and super-microporosity (i.e., approaching the limit of 2.0
373 nm) [1] have also been identified.

The current activated carbon market is the result of intensive research and development in order to enlarge the scope of applications [108–112]. However, not that many resources are economically and/or practically feasible for use as precursors. The most commonly used precursors fall into two main groups: 1) synthetic, including polymers such as polyimide, polyvinyl chloride, and resins; and 2) natural, including wood, fruit stones, and nutshells as well as peat and various ranks of coal. In recent decades, biomass residues have gained interest for use as precursors for activated carbons due to their low cost and ready availability, making them economically feasible for large-scale production. The surface area of commercial activated carbons can reach up to 3000 m^2 g^{-1}, depending on the activation method. Noteworthy, in order to adsorb molecules of different sizes, they must present an appropriate pore size distribution (PSD) (including a large proportion of micropores) [1].

Activated biochars have similar physicochemical characteristics to those for activated carbons made from synthetic or natural materials, and they can provide sustainable, relatively low-cost solutions for mining site remediation and reclamation, water treatment, and industrial applications [113, 114]. These are compelling economic and environmental incentives for further advances in the development of thermochemical conversion methods. Table 1S summarizes the findings on the feedstocks (crop residues, wood biomass, animal litter, sewage sludge, and solid waste) that have been used as precursors for activated biochar production by torrefaction, slow to fast pyrolysis, and gasification under varying conditions. The obtained materials were then activated using different agents and process conditions. The following sections outline the three main activation methods (physical, chemical, and physicochemical) and discuss the porosity of the resultant activated biochars.

4.1. Physical or thermal activation

397 In physical or thermal activation, carbon dioxide (CO_2) or steam (H_2O) are introduced into the
398 atmosphere surrounding the biochar at high temperature and in a limited or zero oxygen
399 environment [115]. The physical agents remove the carbon atoms from the biochar structure. The
400 carbon reacts with the CO_2 or H_2O (entirely in a gas phase) to produce CO (via Boudouard reaction)
401 or CO + H_2, respectively (see Eqs. 1–3) [116].

402 $$C + CO_2 \rightarrow 2CO,\ \Delta H = 159\ \text{kJ mol}^{-1} \quad (1)$$

403 $$C + H_2O \rightarrow CO + H_2,\ \Delta H = 117\ \text{kJ mol}^{-1} \quad (2)$$

404 $$CO + H_2O \leftrightarrow CO_2 + H_2,\ \Delta H = 41\ \text{kJ mol}^{-1} \quad (3)$$

405 Biochar activation with CO_2 removes carbons from the biochar (also called burn-off): as an
406 oxidizing agent, CO_2 penetrates into the internal structure and removes the carbon atoms (Eq. 1),
407 which opens and widens previously inaccessible pores and generates a porous structure [117, 118].
408 Moreover, during devolatilization, or the removal of volatile substances from the solid, the
409 exposure of previously closed pores acts to form new micropores. In addition, existing micropores
410 are widened by a gasification reaction and the collapse of adjacent pore walls to form mesopores
411 [119]. The development of the micropores and mesopores within the structure makes these
412 activated biochars attractive choices for water treatment remediation via adsorption. The potential
413 reasons are the following: 1) mesopores facilitate the mass transfer of solutes into micropores; and
414 2) large-sized pollutant molecules can fit readily into the porous structure [120].

415 Using CO_2 gas activation, (Table 1S), different porous activated biochars were obtained across
416 feedstocks, with surface area ranging from 167 $m^2\ g^{-1}$ for palm kernel shells [121] to 1705 $m^2\ g^{-1}$
417 for corn cob agrowaste, which also presented a combined micro- and mesoporous structure [122].
418 Biochars made from lignocellulosic precursors (e.g., eucalyptus and wattle wood) and activated
419 with CO_2 obtained the highest adsorption capacity, and consequently the highest surface area [123].
420 Similar findings were reported by Grima-Olmedo et al. [124], Guo and Lua [120], Işıtan et al. [125],

421 Jung and Kim [126], and Sricharoenchaikul et al. [127]. The adsorption-desorption curves showed
422 a hysteresis loop, indicating increased mesopore volume, contrary to low temperature (873 K)
423 activation, which obtained predominantly microporosity. Highly porous materials were obtained at
424 1173 K for 1 h in the presence of high CO_2 concentration (100 mL min^{-1}). The optimal parameters
425 enhanced the C–CO_2 reaction, which resulted in higher activated biochar burn-off percentage (83
426 wt.%) and better pore development (S_{BET} up to 1490 m^2 g^{-1}) [1, 123].

427 Using intermediate pyrolysis at 773 and 1073 K and with residence times of 10−30 s, raw oak
428 materials were converted into biochar with surface areas of 107 and 249 m^2 g^{-1}, respectively [126].
429 After activation, increased surface area (up to 1126 m^2 g^{-1}) and micropore development indicated
430 substantial volatile loss during activation at 1173 K and 1 h reaction time. However, at longer
431 residence times (e.g., 2 and 3 h), S_{BET} were significantly lower (1.7 and 2.2 m^2 g^{-1}, respectively).
432 Using CO_2 activation at 1073–1173 K, the volatile matter was removed, resulting in micropore
433 formation due to carbon removal via Boudouard reaction (Eq. 1) [116]. At the same time, with
434 longer residence time, the carbon skeleton of micropores was enlarged to form mesopores as well
435 as macropores. Extending the activation time at such high temperatures eventually destroyed the
436 pore structure of activated biochars [123]. The same findings were observed for activated biochar
437 made from different feedstocks: pistachio nut shells [128], oak wood [126], palm kernel shells
438 [129], pine nut shells [130], and peel waste from *Artocarpus integer* [131].

439 Superheated steam has also been demonstrated a highly effective physical agent, and the most
440 economical option for commercializing activated carbon. Furthermore, it is considered the most
441 environmentally friendly of all the activating agents: it is a relatively simple and clean process, and
442 unlike chemical activation, there is no need for post-treatment to remove by-products. In general,
443 steam is a more reactive physical agent than CO_2 [132–134]. However, the results on the final

444 porosity obtained with different physical activating agents at the same pyro-gasification conditions
445 and feedstock biomass are contradictory. Some authors reported that, compared to CO_2 activation,
446 steam activation produced carbons with a narrower micropore structure due to higher diffusion rates
447 into the pores of the carbon material and the high accessibility of water (as steam) into the
448 micropores, given their smaller size [135–137]. Oppositely, other researchers found that steam-
449 activated carbons presented not only lower micropore volume but also larger external surface area,
450 with pores wider than 2 nm, corresponding to meso- and macropores [126, 133, 134, 138, 139].

451 As presented in Table 1S, biochar activation with superheated steam produced surface areas
452 ranging from 7.1 m^2 g^{-1}, using burcucumber plants as precursor [140], to 1467 m^2 g^{-1}, using date
453 pits [141]. Depending on the feedstock, and even under optimum activation conditions, low surface
454 area and porosity have been reported. Burcucumber plants were pyrolyzed and activated with steam
455 at 573 and 973 K, obtaining low surface area of 1.22 and 7.10 m^2 g^{-1}, respectively [140]. Compared
456 to activated woody biochars (with low ash content), this invasive plant presented very high ash
457 content (28.7 wt.% at 573 K, and 70.7 wt.% at 973 K). Positive correlations have been observed
458 between S_{BET} and ash content, indicating that the surface area as determined by N_2 gas adsorption
459 might represent the surface area of minerals present in biochars [140, 142–147].

460 Similar findings of high porosity development with CO_2 activation have been reported for
461 steam-activated biochars at higher activation temperatures [148, 149], higher steam flow rates [130,
462 150], and residence times up to 1 h [151] and 2 h [130, 131, 141, 148, 149, 151, 152]. Chang et al.
463 [122] conducted a comparative study of activated biochars made from corn agrowaste in the
464 presence of CO_2 or steam. The C–H_2O and C–CO_2 reactions resulted in higher proportions of
465 carbon atom removal. Although CO_2-activated biochars presented higher burn-off and surface area
466 (71 wt.% and 1705 m^2 g^{-1}) compared to steam-activated biochars (59 wt.% and 1315 m^2 g^{-1}), the

latter presented greater microporosity and smaller pore size diameter for the same surface area. This was due to the use of low partial pressure with a mixture of steam and N_2 (40 vol.%), for a more selective attack on the carbon structure. In the case of CO_2 activation, the combination of higher CO_2 concentration and flow rate was less selective [115, 122]. However, no applications were proposed to assess performance in relation to porous structure.

The same findings were reported by Pallarés et al. [153]. The maximum surface area and micropore volume were reached for CO_2-activated barley straw biochar, 789 m^2 g^{-1} and 0.33 cm^3 g^{-1}, while 552 m^2 g^{-1} and 0.23 cm^3 g^{-1} for steam-activated barley straw biochar. It means that the CO_2 material had 43 % higher surface area and micropore volume compared to the steam material. This was explained by the higher reactivity of steam at higher temperatures provoking a pore wide enlarging and increase in mesoporosity. Interesting that this biomass waste contained important amounts of inorganics and consequently CO_2-activated biochar had between 30 and 50 % higher content of inorganics than steam-activated biochar. However, with the increase of activation temperature from 973 to 1073 K, the surface area and total pore volume had an important increase, whereas at 1173 K, low melting temperature silicates appeared which probably filled and blocked the existing pores, losing the activated biochar porous structure.

4.2. Chemical activation

In chemical activation, well known agents such as $ZnCl_2$, H_3PO_4, H_2SO_4, K_2S, HNO_3, K_2CO_3, NaOH, and KOH are used to activate the biochar, resulting in high surface area and appropriate porous structures [154]. In general, acidic chemicals (e.g., H_3PO_4) act as dehydrating agents, whereas bases (e.g., KOH) act as oxidants [155]. In all cases, the first step is to impregnate the biochar with the solid chemical or a solution at various concentrations and amounts. Chemical and physical agents are thought to promote pore development by removing partial carbon atoms from the biochar matrix, which inhibits tar formation and promotes the escape of volatile compounds

[60]. Applying alkali chemicals (e.g., KOH, the most widely used for biochar activation, as seen in Table 1S) followed by heating obtains porosity development via different mechanisms and reactions, according to the equations provided below (Eqs. 4–8). First, the carbon reduces both K and H to their elemental state (Eqs. 4–5). At temperatures above 843 K, this reaction becomes spontaneous. At temperatures above 973 K, K_2CO_3 decomposes into a metallic form of K (boiling-point elevation: 1032 K) and carbon oxides (Eqs. 6–8). The released CO and CO_2 also act as physical agents during activation, thereby contributing to the porosity development. The K_2CO_3 produced in the first step reacts with carbon and releases more gases, such as K_2O, which can subsequently react with carbon to form larger pores. Therefore, the high porosity and surface area of KOH-activated carbons are due to the presence of gases (physical activation) together with metallic compounds (i.e., K) that are intercalated in the carbon lattice [156–159].

$$6KOH + 2C \rightarrow 2K + 3H_2 \uparrow + 2K_2CO_3 \quad (4)$$

$$4KOH + CH_x \rightarrow K_2CO_3 + K_2O + (2+x/2)H_2 \uparrow \quad (5)$$

$$K_2CO_3 \rightarrow K_2O + CO_2 \uparrow \quad (6)$$

$$K_2CO_3 + 2C \rightarrow 2K \uparrow + 3CO \uparrow \quad (7)$$

$$K_2O + C \rightarrow 2K \uparrow + CO \uparrow \quad (8)$$

Applying acid chemicals, such as H_3PO_4, many reactions might take place depending on the different temperature range. From 373 to 673 K, the dehydration of H_3PO_4 is carried out (Eqs. 9–11). From 673 to 973 K, the compound $H_{n+2}P_nO_{3n+1}$ dehydrates and transforms into P_4O_{10} (Eq. 12), which reacts with carbon and reduces to P_4O_6 and CO_2 (Eq. 13), creating new pores as well as widening the existing pores. From 973 to 1073 K, both compounds (P_4O_{10} and/or P_4O_6) might react with the biochar structure generating PH_3 and more gases (CO_2/CO).

$$2H_3PO_4 \rightarrow H_4P_2O_7 + H_2O \quad (9)$$

$$3H_3PO_4 \rightarrow H_5P_3O_{10} + 2H_2O \quad (10)$$

515 $$nH_3PO_4 \rightarrow H_{n+2}P_nO_{3n+1} + (n - 1)H_2O \quad (11)$$

516 $$H_{n+2}P_nO_{3n+1} \rightarrow P_4O_{10} + H_2O \quad (12)$$

517 $$P_4O_{10} + C \rightarrow P_4O_6 + CO_2 \quad (13)$$

518 $$P_4O_{10}/P_4O_6 + CH_x \rightarrow PH_3 + CO_2/CO \quad (14)$$

519 As a result, chemically activated biochars have higher porosity compared to physically activated
520 biochars. The highest surface area (i.e., 3167 m^2 g^{-1}) was reported for activated biochar made from
521 mesquite trees using a KOH:biochar mass ratio of 5:1 at 1073 K [160], followed by spruce
522 whitewood at 1148 K for 2 h (S_{BET} = 2673 m^2 g^{-1}) [12]. Woody residues, are therefore, good
523 lignocellulosic precursors for activated carbon production. The main advantages are high carbon
524 and low inorganic material contents, relatively high volatile content, and widespread availability.
525 At the same time, as deforestation accelerates, the scientific community is looking at agricultural
526 wastes for activated biochar production. For example, surface areas for KOH-activated biochars
527 were greater than 2500 m^2 g^{-1} for distiller-dried grains treated at high temperatures (1223 and 1323
528 K for 3 h) [161] and for rice straw (973 K for 1 h) [162].

529 The activation temperature and impregnation ratio (defined as the mass ratio of the chemical
530 agent to the biochar), play influential roles in porosity and surface area development, and hence the
531 capacity to adsorb pollutants. Biochar prepared from safflower seed press cake at 773 K and
532 chemically activated with $ZnCl_2$ increased in surface area from 249 to 802 m^2 g^{-1} with increased
533 temperature from 873 to 1173 K [163]. Similar findings were reported when the $ZnCl_2$:biochar
534 impregnation mass ratio was increased from 1:1 to 4:1, producing increased surface areas of 620
535 and 802 m^2 g^{-1}, respectively. The shape of the N_2 adsorption-desorption isotherm for chemically
536 activated biochars indicated a predominantly microporous structure with some mesoporosity (up to
537 30 %; type I and IV isotherms according to IUPAC classification [163]). FTIR analysis showed a

538 strong presence of aliphatic groups (e.g., –CH, –CH_2 or –CH_3), indicating decreased proportions of
539 alcohols, phenols, and ethers, possibly due to the extraction of –H and –OH groups from aromatic
540 rings during impregnation and thermal treatment [163].

541 High ash content (up to 66 wt.%) improved the porosity of chemically activated biochar made
542 from sewage sludge due to the presence of inorganics. Three kinds of sludge were recovered from
543 a wastewater treatment plant, pyrolyzed at 973 K under nitrogen flow, and activated using KOH at
544 1:1 KOH:biochar mass ratio. Sewage sludge biomass structure is highly complex compared to other
545 biomass types (e.g., lignocellulosic wastes). The carbon content ranged from 26 to 31 wt.%, and up
546 to 40 wt.% was constituted of inorganic species. It was also observed that, unlike physical
547 activation, the mineral matter was involved in the KOH activation, for a positive effect on porosity
548 development. Biologic sewage sludge obtained surface areas in the range of 1900 m^2 g^{-1}. At high
549 temperatures, KOH acted not only as an activating agent for sludge-based precursors, it also
550 produced an alkaline fusion with the inorganic matter present in the sewage sludge, thereby
551 catalyzing the activation reaction. The nitrogen from microorganisms was maintained even after
552 treatment at 973 K, producing nitrogenated carbonaceous materials. This type of functionalized
553 sludge-derived activated biochar could be suitable for a wide range of applications, including liquid
554 adsorption as well as electrochemistry and catalysis [55].

555 Generally, the higher the impregnation ratio, the higher the porosity of the activated biochar, as
556 confirmed by Angın et al. [164], Mao et al. [165], and Zhang et al. [166]. Biochars made from pork
557 bones were activated separately with H_2SO_4 and H_3PO_4 at 1073 K. Using H_2SO_4 as the chemical
558 agent, the lowest acid:biochar impregnation mass ratio increased the surface area by about 80 %
559 (up to 140 m^2 g^{-1}) compared to untreated biochar (76 m^2 g^{-1}). In contrast, using H_3PO_4 as the
560 activating agent, surface area decreased sharply with higher impregnation ratio. At the lowest

561 impregnation ratio (0.2 mmol g^{-1}), S_{BET} was around 136 m^2 g^{-1}, and at 20 mmol g^{-1} it dropped
562 sharply to 3.2 m^2 g^{-1}. Chemical activation with H_3PO_4 had an aggressive effect on the final
563 materials. XRD analysis revealed that, after acid and heat treatment, various phosphate compounds
564 were produced, including $CaHPO_4.2H_2O$, $Ca(H_2PO_4)_2.2H_2O$, and $Ca_3(PO_4)_2$. The removal of
565 $CaCO_3$ was also confirmed by FTIR analysis. SEM images revealed significant cracking of the
566 precursor particles, as confirmed by the drastic reduction in pore volume and surface area. This
567 dramatic change in the structure and composition of activated biochar could be attributed to an
568 amorphous and thermolabile structure that collapsed during thermal treatment [167].

569 **4.3. Physicochemical activation**

570 Physicochemical activation is also used to produce activated biochar. In such case, the biochar
571 is chemically impregnated and then heat treated in the presence of a physical agent (CO_2 or steam)
572 in an inert atmosphere. Wu and Tseng [168] obtained outstanding surface areas (1371–2821 m^2 g^{-}
573 ^{1}), with total pore volumes from 0.81 to 1.73 cm^3 g^{-1}, by impregnating fir wood biochar with KOH
574 and then activating at 1053 K in the presence of CO_2 gas. The adsorbed nitrogen volume depended
575 strongly on the CO_2 gasification duration. The activation process produced porosity at the surface
576 of the holes, resulting in the formation of finer walls with clear corner lines, as observed in SEM
577 images.

578 Rostamian et al. [169] conducted a comparative study of activated biochars derived from rice
579 husks using three activation methods: chemical (using KOH), physical (using steam), and the two
580 combined at 1073 K. The raw material presented very low surface area (1.4 m^2 g^{-1}), which increased
581 significantly after pyrolysis and subsequent activation to 2201 (chemical), 317 (physical), and 1169
582 m^2 g^{-1} (the two combined). The KOH-activated biochar showed a well developed porous structure
583 with smaller pore diameters (e.g., 1.7 nm) compared to 2.2 nm for steam-activated biochar. Notably,

584 physicochemical activation (the most expensive method) produced less satisfactory pore structure
585 development compared to chemical activation. The authors suggested that the introduction of both
586 agents (KOH and steam) may have caused the pore walls to thin and collapse, or else to form very
587 thin pores or ultramicropores that were inadequate for N_2 adsorption [169]. Moreover, the rice
588 husks had high ash content (47 wt.%), which may have interfered with the reaction mechanisms
589 between steam and the organic matter in the biochar.

590 Compared to physically activated materials, biochars that have been chemically or
591 physicochemically activated present higher porosity, and are suitable for many more applications
592 (Table 1S). This is because porosity is a key factor for adsorptive capacity. Materials with high
593 surface area (> 1000 m^2 g^{-1}) and high specific pore size distribution such as ultramicropores,
594 micropores, or micropores with a certain degree of mesoporosity have been used for gas adsorption
595 (CO_2, H_2S), as catalyst supports, and as components of supercapacitors, electric double-layer
596 capacitors (EDLC), and lithium batteries. Table 1S also presents the various applications of
597 activated biochars with high (> 1000 m^2 g^{-1}) and moderate (300−800 m^2 g^{-1}) surface areas for
598 immobilizing aromatic and heavy metals in soil and for absorbing contaminants in water, including
599 organic (iodine, methylene blue, herbicide atrazine, dyestuff, phenol, acid yellow 36,
600 sulfamethazine, ibuprofen, endocrine disrupting compounds, and pharmaceuticals) and inorganic
601 contaminants (Cu^{2+}, Cd^{2+}, Zn^{2+}, Ni^{2+}, Hg^{2+}, Cu^{2+}, As^{3+}). The main mechanism involved in
602 contaminant removal is physical sorption (pore diffusion). Depending on the contaminant and the
603 surface chemistry and physicochemical characteristics of the activated biochar, other mechanisms
604 may also be involved. These include ion exchange, metal electrostatic attraction, and precipitation
605 in activated biochar–inorganic contaminant interactions; and electrostatic interactions in activated

606 biochar–organic contaminant interactions. These findings underscore the advantages of developing
607 highly porous biochars with tailored physicochemical properties for a wide variety of end uses.

608 **4.4. Effects of pyro-gasification conditions on the porosity of activated biochar**

609 4.4.1. Pyro-gasification temperature

610 Few studies on activated biochar production have focused on the effects of pyro-gasification
611 temperature on the final porosity (Table 1S). Fig. 2 presents the surface areas of biochars made
612 from various feedstocks as a function of pyro-gasification temperature using: a) CO_2 or steam
613 activation, and b) chemical activation with NaOH or KOH. Three types of materials, lignocellulosic
614 (residues from white birch and black spruce, almond shells, pistachio nut shells, nutshells and oil
615 palm shells) [125, 170–172], broiler litter (rich in nitrogen, sulfur, and inorganics) [173], and plants
616 (rich in inorganics) [140], were activated in the presence of CO_2 or steam at different pyro-
617 gasification temperatures (Fig. 2 a)). In a comparison of lignocellulosic materials activated in the
618 presence of CO_2 at the same temperature (1173 K), activated biochars made from nut shells
619 presented higher porosity compared to pistachio nuts and oil palm shells (ash contents below 2
620 wt.%). Only insignificant differences were observed in surface area across pyro-gasification
621 temperatures, except at very low (523−573 K) pyrolysis temperatures, where lower porosity was
622 found for pistachio nut shells compared to the 673−1173 K range [171]. Biochars with almond
623 shells as lignocellulosic precursor were subjected to successive thermal treatments at low (3−4 K
624 min^{-1} at 548−673 K) and high (3000 K min^{-1} at 1123 K) heating rates. Activation at 1053 K in the
625 presence of CO_2 produced highly porous materials, but no significant differences in surface area
626 were observed across pyro-gasification temperatures [170]. Other authors found that activation
627 temperature was the most influential variable for increasing the surface area. Recently, Işıtan *et al.*
628 [125] used regression analysis to examine the impact of pyrolysis and activation temperature on the

surface area of activated pistachio nut shell biochar and found that increasing the temperature from 1073 to 1173 K in the presence of CO_2 produced more than 300 m^2 g^{-1} increased surface area for all pre-carbonization temperatures (723, 823, 923 K). The regression analysis indicated that pyrolysis temperature had no significant impact on the final surface area or pore volume. Similarly, the influence of torrefaction/fast pyrolysis of white birch and black spruce on the porosity development of CO_2-activated biochars was statistically exanimated by Braghiroli et al. [174]. The pyro-gasification temperature was varied from 588 to 727 K and the activation temperature varied from 973 to 1173 K. It was concluded that the first step pyro-gasification had less impact on the porosity of activated biochars while the activation temperature was the major variable to optimize their surface area. By increasing the activation temperature from 973 to 1173 K, the average surface area of CO_2-activated biochars increased to nearly 120 m^2 g^{-1}.

In activated biochars prepared from other types of materials (plants and broiler litter) having different morphological and chemical compositions from those for lignocellulosic precursors, lower porosity was obtained due to the higher ash content (up to 71 wt.% for steam-activated plant biochars) [140] compared to woody biochars (< 5 wt.%). Using broiler litter feedstock, the same surface area of 335 m^2 g^{-1} was measured for two biochars produced at pyrolysis temperatures of 623 and 973 K followed by activation at 1073 K in the presence of steam. Pyrolysis temperature showed no effect on the porosity of either material, but the activated biochar pyrolyzed at 973 K presented higher capacity for herbicide atrazine sorption due to its higher aromacity [173].

In sum, biochars that were activated in the presence of physical agents presented no significant variations in porosity as a function of pyro-gasification temperature for these three groups of materials. The variation in surface area across materials was due to the feedstock quality: differences in lignocellulosic component contents, morphology, and chemical structure. These

652 findings indicate that the use of low-temperature pyro-gasification (e.g., 673 K) to produce
653 physically activated biochars could have economic benefits, notably lower energy required to
654 improve product quality.

655 The changes in surface area for chemically activated biochars (at almost the same activation
656 temperature: 1073 or 1098 K) as a function of the pyro-gasification temperature differ from the
657 changes for physically activated biochars (Fig. 2 a) and 2 b)). Highly porous materials were
658 obtained by chemical activation (S_{BET} up to 2800 m^2 g^{-1}), and high ash content had a positive effect
659 on increased porosity [175]. For instance, rice husks contain inorganics (~ 15 wt.%, including silica,
660 potassium, and calcium) that interact with NaOH via a complex mechanism, which in turn fosters
661 gasification reactions and hence pore development. Increasing the torrefaction temperature from
662 493 to 553 K contributed to increase the porosity of rice husk torrefied materials. Using 553 K
663 torrefaction temperature and subsequent activation, the materials presented a surface area increase
664 of 2679 m^2 g^{-1} compared to 2297 m^2 g^{-1} when prepared at 493 K.

665 However, it is noteworthy that surface area decreased drastically with increased pyro-
666 gasification temperature for loblolly pine chips [176] and rice straw [162] as precursors. Increased
667 pyro-gasification temperature from 573 to 973 K had a negative effect on the porosity of NaOH-
668 activated wood chip biochars (surface area reduced from 1250 to 57 m^2 g^{-1}) [176]. High pyrolysis
669 temperature (1273 K) also lowered the surface area of KOH-activated rice straw biochar compared
670 to 973 K (2200 vs. 1050 m^2 g^{-1}) [162]. At low pyro-gasification temperatures (573 K), activated
671 biochars had lower aromacity and smaller-sized aromatic clusters (non-protonated carbon content)
672 but higher amounts of alkyl carbons and volatile matter, which almost completely disappeared after
673 activation, resulting in the formation of highly porous materials. In contrast, at high pyro-
674 gasification temperature, activated biochar had higher aromacity and larger-sized aromatic clusters.

675 This provided a more rigid, stable, and inactive carbon structure (with condensed aromatic
676 structures) with fewer oxygen-containing groups at the edges of the carbon layers [176, 177]. This
677 structure was resistant to thermal degradation, even when using severe chemicals (e.g., NaOH),
678 which inhibited porosity development. In light of these findings, studies are needed to determine
679 optimal pyro-gasification temperatures when preparing feedstock precursors for activated biochar
680 production, and particularly via chemical activation.

681 #### 4.4.2. Residence time and heating rate

682 Residence time (Fig. 3 a)) and heating rate (Fig. 3 b)) are two parameters that have been
683 investigated for their impact on the porosity of activated biochars. The effects of various residence
684 times on the porosity of activated biochars were assessed for pistachio nut and oil palm shells (ash
685 contents < 1 %) pyrolyzed at 773 and 873 K, respectively, and activated at 1173 K (Fig. 3 a)).
686 Longer residence time (from 0.5 to 2 h) during slow pyrolysis progressively increased the porosity
687 due to the improved rudimentary pore structure of the biochars with the release of volatile matter.
688 However, at longer residence times (i.e., > 2 h), activated biochars presented lower porosity [141,
689 171, 172]. Hamza et al. [121] also found that the surface area of activated oil palm shell biochars
690 prepared at 1073 K for 2 to 4 h was reduced from 167 to 138 m^2 g^{-1}. Prolonged residence time
691 results in secondary reactions, notably tar reactions on the biochar surface and tar charring. Higher
692 and prolonged heat during pyrolysis causes the low-molecular-weight volatiles to increase, soften,
693 and sinter, hence forming an intermediate melt [172]. This melt formation blocks off some pores in
694 the chars, resulting in lower porosity development during activation. However, for other feedstock
695 types, such as date pits [141], the longer the residence time (from 0.5 to 4 h), the higher the porosity
696 of the final material (from 840 to 1467 m^2 g^{-1}).

697 The influence of heating rate on the porosity of activated biochars was assessed for pistachio
698 nut and oil palm shells as precursors (particle size: 2−2.8 nm) pyrolyzed at 773 and 873 K,
699 respectively, and activated at 1173 K [171, 172] (Fig. 3 b)). When the heating rate was increased
700 from 5 to 10 K min^{-1}, both materials increased in surface area and subsequently decreased with
701 increased heating rate from 15 to 50 K min^{-1}. At the highest heating rate (50 K min^{-1}), the materials
702 exhibited decreased surface area, because the shorter residence time was insufficient to maximize
703 pore development. For both feedstocks, the optimal heating rate for biochar production was 10 K
704 min^{-1}.

705 To summarize, only a few studies have assessed the impact of pyro-gasification conditions on
706 the porosity of activated biochars. This calls for a comprehensive optimization approach in order
707 to minimize the energy requirements for biomass thermochemical conversion and maximize the
708 final porosity.

709 #### 4.4.3. Reactor design

710 In the overview of the research on activated biochars (Table 1S), one could see that the majority
711 of biomass precursors were transformed into biochar with laboratory-scale furnaces, which have
712 highly controllable parameters. However, some studies used the products or by-products of small-
713 to large-scale pyro-gasification reactor operations as precursors for activated materials. These
714 activated biochars were synthesized in a two-step process: 1) torrefaction, slow to fast pyrolysis,
715 gasification, or kiln charcoal production; and 2) activation in another laboratory-scale furnace
716 reactor in the presence of physical and chemical agents to develop the porosity. In a pioneering
717 study, Azargohar and Dalai [178] used biochars produced by a commercial renewable bio-oil
718 production company. Fast pyrolysis of sawdust biochar yielded 70 % bio-oil, 20 % biochar, and 10
719 % syngas. The biochar was then chemically activated to produce an added-value biochar with

720 surface area up to 1578 m^2 g^{-1}. Zhang et al. [179] used a fluidized sand-bed reactor at 7 kg h^{-1}
721 residue feed rate and 773 K to transform biomass waste (oak wood, corn hulls, and corn stover)
722 into biochar, then activated it with CO_2 at 1073 K to obtain surface areas up to 1010 m^2 g^{-1}.
723 Although both these studies obtained highly porous materials, they used small-scale activation
724 furnaces: a fixed-bed tubular reactor and a quartz tube reactor vessel, respectively.

725 Gasification reactors, including a downdraft gasifier and a fluidized bed gasifier, were used to
726 prepare biochars that were subsequently activated [180]. In the downdraft (co-current) gasifier, the
727 fuel and the product gas flow in the same direction, forming tar-cracking zones in the reactor at
728 higher temperatures. The main components of the downdraft gasifier include a cyclone-based
729 pyrolysis section followed by a fixed-bed gasification section [181]. The fluidized bed consists of
730 a cylindrical reactor column with a bed of inert material, such as sand. The gasifying mechanism is
731 fluidization: the fuel combined with the inert bed material behaves like a fluid. This is obtained by
732 forcing a gas (the fluidization medium) through the solid inventory in the reactor [182]. The
733 biochars generated by the downdraft gasifier and fluidized bed reactor had surface areas of 64 and
734 2 m^2 g^{-1}, respectively. After KOH-activation in a laboratory furnace, surface areas increased to 900
735 and 200 m^2 g^{-1}, respectively [180]. These findings indicate that the configurations of the two
736 gasifiers created different gasification conditions, which can strongly influence the porosity of the
737 end product.

738 Studies on the use of biochar as a by-product from large-scale pyro-gasification operations have
739 demonstrated that the synthesized material have characteristics that are suitable for many end uses.
740 In addition, further activation can develop comparable porosity to that for materials prepared in
741 small-scale furnaces, which have more controllable parameters due to the small amount of
742 stationary precursor used. Together, the pyro-gasification conditions (e.g., reactor design,

743 temperature, pyrolysis type, heating rate) and the feedstock (with differing morphologies and
744 chemical structures) wield a significant influence on the characteristics of the final activated
745 biochars. However, the conditions could be optimized to maximize the porosity and lower the
746 energy required to achieve material quality. The current challenge in activated biochar production
747 is that only laboratory-scale furnaces have been tested to date. Braghiroli et al. [174] produced
748 highly porous physically and chemically activated biochars made from wood residues through a
749 torrefaction/fast pyrolysis industrial furnace (Airex Energy, Canada, 250 kg h^{-1}) and a prototype
750 activation furnace (slow pyrolysis in a shaftless screw conveyor reactor, 1 kg h^{-1}). One promising
751 direction would be to combine both furnaces having flexible and scalable activation processes with
752 high temperatures (up to 1173 K) and long residence times (1 h minimum) at various heating rates.
753 Biorefineries could also improve the efficiency of their thermochemical conversion operations and
754 diversify their product range to include economically attractive biochars, bio-oil, syngas, and
755 activated biochars.

756 **5. Conclusions and future research directions**

757 This extensive literature review addresses the influence of pyro-gasification and activation
758 conditions on the properties of activated biochars derived from a large variety of feedstocks. The
759 main conclusions are summarized as follows:

760 1. The physicochemical properties of lignocellulosic materials used as feedstock precursors for
761 activated biochar production vary widely compared to the properties of other materials, such as
762 animal manure, crop residues, food waste, algae, and wastewater sludge. Because the biochar's
763 chemical composition strongly influences the properties of the activated material, biochars must
764 be physicochemically characterized to determine their suitability for specific applications.

765 2. The pyro-gasification conditions (including temperature, residence time, heating rate, and
766 reactor design) strongly influence the textural properties of the activated biochar. Interestingly,
767 however, and compared to chemical activation, variations in pyro-gasification temperature (in
768 the 673−1173 K range) have not substantially affected porosity development in physically
769 activated biochars. Nevertheless, very few feedstocks have been assessed, and studies are
770 needed to optimize processing conditions. Improved process efficiency in relation to product
771 quality would minimize energy requirements (e.g., low pyro-gasification temperatures) without
772 impacting the porosity of the end product.

773 3. The activation conditions play an important role in the porosity development of activated
774 biochars. High temperatures (up to 1173 K), residence times from 1 to 2 h, higher steam or CO_2
775 gas flow rates, and optimal chemical agent:biochar mass ratios produced activated biochars
776 with suitable porosity structures for specific applications. In addition, longer residence times,
777 higher heating rates, and higher proportions of physical and chemical agents were also found to
778 drastically reduce the porosity of activated biochars, resulting in the formation of
779 ultramicropores or macropores (inaccessible by N_2 adsorption analysis), or alternatively, the
780 collapse of amorphous and thermolabile structures in activated biochars during thermal
781 treatment. It is therefore recommended to optimize the activation parameters.

782 4. Chemical activation with KOH was demonstrated effective to obtain highly porous biochars
783 (S_{BET} up to 3000 m^2 g^{-1}) derived from several feedstock types, and particularly lignocellulosic
784 materials. Agricultural waste residues appear to be promising precursors, as KOH activation
785 produced biochar surface areas up to 2500 m^2 g^{-1}. However, further studies are needed to clarify
786 the structure of biomass precursors as well as the activation mechanisms. Work is also needed
787 to improve the final porosity, a critical property for expanded end uses.

5. Biochar activation is a promising method to improve the textural properties of new, renewable biomaterials for use in a wide range of fields, including catalysis, electrochemistry, energy storage, and contaminant removal from drinking water and wastewater. Notably, this review did not address the cost of activated biochar production. Future studies could explore the use of flexible and scalable activation methods with higher temperature capacity (up to 1173 K), longer residence times (e.g., 1 h), and varied heating rates. Advances in this area would significantly benefit the biorefinery industry and the environment through the development of sustainable, low-cost biomaterials for a wide range of applications.

Acknowledgments

This project was funded by the *Ministère de l'Économie, de la Science et de l'Innovation du Québec* (Québec's ministry of economy, science, and innovation), the Natural Sciences and Engineering Research Council of Canada (NSERC), the *Canada Research Chair Program*, the *Cégep de l'Abitibi-Témiscamingue* (Abitibi-Témiscamingue College), and the *Centre Technologique des Résidus Industriels* (Industrial Waste Technology Center) under a partnership with Airex Energy. The first author, Dr. Flavia Lega Braghiroli, also sincerely acknowledges NSERC financial support via a Banting Postdoctoral Fellowship (2017–2019).

References

1. Marsh, H., Rodríguez-Reinoso, F.: Activated carbon. Elsevier, Amsterdam, NL (2006)
2. IBI: International Biochar Initiative, http://www.biochar-international.org/
3. Subba Rao, D.V., Gouricharan, T.: Coal Processing and Utilization. CRC Press, London, UK (2016)
4. Homagain, K., Shahi, C., Luckai, N., Sharma, M.: Life cycle cost and economic assessment of biochar-based bioenergy production and biochar land application in Northwestern Ontario, Canada. For. Ecosyst. 3, 1–10 (2016). doi:10.1186/s40663-016-0081-8
5. Hu, Q., Shao, J., Yang, H., Yao, D., Wang, X., Chen, H.: Effects of binders on the properties of bio-char pellets. Appl. Energy. 157, 508–516 (2015). doi:10.1016/j.apenergy.2015.05.019
6. Ohsowski, B.M., Dunfield, K., Klironomos, J.N., Hart, M.M.: Plant response to biochar, compost, and mycorrhizal fungal amendments in post-mine sandpits: synergism among soil amendments. Restor. Ecol. 1–10 (2017). doi:10.1111/rec.12528
7. Peltz, C.D., Harley, A.: Biochar Application for Abandoned Mine Land Reclamation. In: Guo, M., He, Z., and Uchimiya, S.M. (eds.) Agricultural and Environmental Applications of Biochar: Advances and Barriers. pp. 325–340. Soil Science Society of America, Inc. (2016)
8. Ahmed, A., Kurian, J., Raghavan, V.: Biochar influences on agricultural soils, crop production, and the environment: a review. Environ. Rev. 24, 495–502 (2016). doi:10.1139/er-2016-0008
9. Ahmad, M., Lee, S.S., Lee, S.E., Al-Wabel, M.I., Tsang, D.C.W., Ok, Y.S.: Biochar-induced changes in soil properties affected immobilization/mobilization of metals/metalloids in contaminated soils. J. Soils Sediments. 17, 717–730 (2017). doi:10.1007/s11368-015-1339-4
10. TechSci Research: Global activated carbon market by type (powdered activated carbon, granular activated carbon and others), by raw material (wood, coconut shells, coal and others), by application, competition forecast and opportunities, 2011-2021 (2016) https://www.techsciresearch.com/news/1203-activated-carbon-market-size-set-to-cross-4-9-billion-by-2021.html
11. Gupta, R.K., Dubey, M., Kharel, P., Gu, Z., Fan, Q.H.: Biochar activated by oxygen plasma for supercapacitors. J. Power Sources. 274, 1300–1305 (2015). doi:10.1016/j.jpowsour.2014.10.169
12. Dehkhoda, A.M., Gyenge, E., Ellis, N.: A novel method to tailor the porous structure of KOH-activated biochar and its application in capacitive deionization and energy storage. Biomass Bioenergy. 87, 107–121 (2016). doi:10.1016/j.biombioe.2016.02.023
13. Zhang, H., Yu, F., Kang, W., Shen, Q.: Encapsulating selenium into macro-/micro-porous biochar-based framework for high-performance lithium-selenium batteries. Carbon. 95, 354–363 (2015). doi:10.1016/j.carbon.2015.08.050
14. Li, Y., Ruan, G., Jalilov, A.S., Tarkunde, Y.R., Fei, H., Tour, J.M.: Biochar as a renewable source for high-performance CO_2 sorbent. Carbon. 107, 344–351 (2016). doi:10.1016/j.carbon.2016.06.010
15. Nguyen, M.-V., Lee, B.-K.: A novel removal of CO_2 using nitrogen doped biochar beads as a green adsorbent. Chall. Environ. Sci. Eng. 104, Part B, 490–498 (2016). doi:10.1016/j.psep.2016.04.007

16. Zhu, L., Yin, S., Yin, Q., Wang, H., Wang, S.: Biochar: a new promising catalyst support using methanation as a probe reaction. Energy Sci. Eng. 3, 126–134 (2015). doi:10.1002/ese3.58
17. Shen, B., Chen, J., Yue, S., Li, G.: A comparative study of modified cotton biochar and activated carbon based catalysts in low temperature SCR. Fuel. 156, 47–53 (2015). doi:10.1016/j.fuel.2015.04.027
18. Park, C.M., Han, J., Chu, K.H., Al-Hamadani, Y.A.J., Her, N., Heo, J., Yoon, Y.: Influence of solution pH, ionic strength, and humic acid on cadmium adsorption onto activated biochar: experiment and modeling. J. Ind. Eng. Chem. 48, 186–193 (2017). doi:10.1016/j.jiec.2016.12.038
19. Mondal, S., Aikat, K., Halder, G.: Ranitidine hydrochloride sorption onto superheated steam activated biochar derived from mung bean husk in fixed bed column. J. Environ. Chem. Eng. 4, 488–497 (2016). doi:10.1016/j.jece.2015.12.005
20. Ahmad, M., Rajapaksha, A.U., Lim, J.E., Zhang, M., Bolan, N., Mohan, D., Vithanage, M., Lee, S.S., Ok, Y.S.: Biochar as a sorbent for contaminant management in soil and water: a review. Chemosphere. 99, 19–33 (2014). doi:10.1016/j.chemosphere.2013.10.071
21. Bolan, N.S., Thangarajan, R., Seshadri, B., Jena, U., Das, K.C., Wang, H., Naidu, R.: Landfills as a biorefinery to produce biomass and capture biogas. Biorefineries. 135, 578–587 (2013). doi:10.1016/j.biortech.2012.08.135
22. Bridgwater, A.V.: Review of fast pyrolysis of biomass and product upgrading. Biomass Bioenergy. 38, 68–94 (2012). doi:10.1016/j.biombioe.2011.01.048
23. Brown, R.: Biochar Production Technology. In: Lehmann, J. and Joseph, S. (eds.) Biochar for Environmental Management: Science and Technology. pp. 127–139, London, UK (2009)
24. Laird, D.A., Brown, R.C., Amonette, J.E., Lehmann, J.: Review of the pyrolysis platform for coproducing bio-oil and biochar. Biofuels Bioprod. Biorefining. 3, 547–562 (2009). doi:10.1002/bbb.169
25. Libra, J.A., Ro, K.S., Kammann, C., Funke, A., Berge, N.D., Neubauer, Y., Titirici, M.-M., Fühner, C., Bens, O., Kern, J., Emmerich, K.-H.: Hydrothermal carbonization of biomass residuals: a comparative review of the chemistry, processes and applications of wet and dry pyrolysis. Biofuels. 2, 71–106 (2011). doi:10.4155/bfs.10.81
26. Zabaniotou, A., Rovas, D., Libutti, A., Monteleone, M.: Boosting circular economy and closing the loop in agriculture: case study of a small-scale pyrolysis–biochar based system integrated in an olive farm in symbiosis with an olive mill. Environ. Dev. 14, 22–36 (2015). doi:10.1016/j.envdev.2014.12.002
27. Antal, M.J., Grønli, M.: The art, science, and technology of charcoal production. Ind. Eng. Chem. Res. 42, 1619–1640 (2003). doi:10.1021/ie0207919
28. Azargohar, R., Nanda, S., Kozinski, J.A., Dalai, A.K., Sutarto, R.: Effects of temperature on the physicochemical characteristics of fast pyrolysis bio-chars derived from Canadian waste biomass. Fuel. 125, 90–100 (2014). doi:10.1016/j.fuel.2014.01.083
29. Ronsse, F.: Biochar Production. In: Bruckman, V.J., Apaydin Varol, E., Uzun, B.B., and Liu, J. (eds.) Biochar: a regional supply chain approach in view of climate change mitigation. pp. 199–226. Cambridge University Press, Cambridge (2016)
30. Park, W.C., Atreya, A., Baum, H.R.: Experimental and theoretical investigation of heat and mass transfer processes during wood pyrolysis. Combust. Flame. 157, 481–494 (2010). doi:10.1016/j.combustflame.2009.10.006

31. Venderbosch, R., Prins, W.: Fast pyrolysis technology development. Biofuels Bioprod. Biorefining. 4, 178–208 (2010). doi:10.1002/bbb.205
32. Arazo, R.O., Genuino, D.A.D., de Luna, M.D.G., Capareda, S.C.: Bio-oil production from dry sewage sludge by fast pyrolysis in an electrically-heated fluidized bed reactor. Sustain. Environ. Res. 27, 7–14 (2017). doi:10.1016/j.serj.2016.11.010
33. Vassilev, S.V., Baxter, D., Andersen, L.K., Vassileva, C.G., Morgan, T.J.: An overview of the organic and inorganic phase composition of biomass. Fuel. 94, 1–33 (2012). doi:10.1016/j.fuel.2011.09.030
34. Pandey, A., Bhaskar, T., Stöcker, M., Sukumaran, R. eds: Recent Advances in Thermochemical Conversion of Biomass. Elsevier, Amsterdam, NL (2015)
35. Tang, W.K., Neill, W.K.: Effect of flame retardants on pyrolysis and combustion of α-cellulose. J. Polym. Sci. Part C Polym. Symp. 6, 65–81 (2007). doi:10.1002/polc.5070060109
36. Babu, B.V.: Biomass pyrolysis: a state-of-the-art review. Biofuels Bioprod. Biorefining. 2, 393–414 (2008). doi:10.1002/bbb.92
37. Mohan, D., Pittman Jr., Charles U., Steele, P.H.: Pyrolysis of wood/biomass for bio-oil: a critical review. Energy Fuels. 20, 848–889 (2006). doi:10.1021/ef0502397
38. Soltes, E.J., Elder, T.J.: Pyrolysis. In: Goldstein, I.S. (ed.) Organic Chemicals from Biomass. pp. 63–95. CRC Press, Boca Raton, FL (1981)
39. Chu, S., Subrahmanyam, A.V., Huber, G.W.: The pyrolysis chemistry of a β-O-4 type oligomeric lignin model compound. Green Chem. 15, 125–136 (2013). doi:10.1039/C2GC36332A
40. Mu, W., Ben, H., Ragauskas, A., Deng, Y.: Lignin pyrolysis components and upgrading—technology review. BioEnergy Res. 6, 1183–1204 (2013). doi:10.1007/s12155-013-9314-7
41. Ingram, L., Mohan, D., Bricka, M., Steele, P., Strobel, D., Crocker, D., Mitchell, B., Mohammad, J., Cantrell, K., Pittman, C.U.: Pyrolysis of wood and bark in an auger reactor: physical properties and chemical analysis of the produced bio-oils. Energy Fuels. 22, 614–625 (2008). doi:10.1021/ef700335k
42. Jahirul, M., Rasul, M., Chowdhury, A., Ashwath, N.: Biofuels production through biomass pyrolysis —A technological review. Energies. 5, 4952–5001 (2012). doi:10.3390/en5124952
43. Li, S., Lyons-Hart, J., Banyasz, J., Shafer, K.: Real-time evolved gas analysis by FTIR method: an experimental study of cellulose pyrolysis. Fuel. 80, 1809–1817 (2001). doi:10.1016/S0016-2361(01)00064-3
44. Shafizadeh, F., Fu, Y.L.: Pyrolysis of cellulose. Carbohydr. Res. 29, 113–122 (1973). doi:10.1016/S0008-6215(00)82074-1
45. Lin, Y.-C., Cho, J., Tompsett, G.A., Westmoreland, P.R., Huber, G.W.: Kinetics and mechanism of cellulose pyrolysis. J. Phys. Chem. C. 113, 20097–20107 (2009). doi:10.1021/jp906702p
46. Mettler, M.S., Paulsen, A.D., Vlachos, D.G., Dauenhauer, P.J.: Pyrolytic conversion of cellulose to fuels: levoglucosan deoxygenation via elimination and cyclization within molten biomass. Energy Environ. Sci. 5, 7864–7868 (2012). doi:10.1039/C2EE21305B
47. Ronsse, F., Bai, X., Prins, W., Brown, R.C.: Secondary reactions of levoglucosan and char in the fast pyrolysis of cellulose. Environ. Prog. Sustain. Energy. 31, 256–260 (2012). doi:10.1002/ep.11633
48. Shen, D., Xiao, R., Gu, S., Luo, K.: The pyrolytic behavior of cellulose in lignocellulosic biomass: a review. RSC Adv. 1, 1641–1660 (2011). doi:10.1039/C1RA00534K

49. Vinu, R., Broadbelt, L.J.: A mechanistic model of fast pyrolysis of glucose-based carbohydrates to predict bio-oil composition. Energy Environ. Sci. 5, 9808–9826 (2012). doi:10.1039/C2EE22784C
50. Huang, J., Liu, C., Tong, H., Li, W., Wu, D.: Theoretical studies on pyrolysis mechanism of xylopyranose. Comput. Theor. Chem. 1001, 44–50 (2012). doi:10.1016/j.comptc.2012.10.015
51. Shen, D.K., Gu, S., Bridgwater, A.V.: Study on the pyrolytic behaviour of xylan-based hemicellulose using TG–FTIR and Py–GC–FTIR. J. Anal. Appl. Pyrolysis. 87, 199–206 (2010). doi:10.1016/j.jaap.2009.12.001
52. Shen, D.K., Gu, S., Bridgwater, A.V.: The thermal performance of the polysaccharides extracted from hardwood: cellulose and hemicellulose. Carbohydr. Polym. 82, 39–45 (2010). doi:10.1016/j.carbpol.2010.04.018
53. Patwardhan, P.R., Satrio, J.A., Brown, R.C., Shanks, B.H.: Influence of inorganic salts on the primary pyrolysis products of cellulose. Bioresour. Technol. 101, 4646–4655 (2010). doi:10.1016/j.biortech.2010.01.112
54. Debiagi, P.E.A., Trinchera, M., Frassoldati, A., Faravelli, T., Vinu, R., Ranzi, E.: Algae characterization and multistep pyrolysis mechanism. J. Anal. Appl. Pyrolysis. 128, 423–436 (2017). doi:10.1016/j.jaap.2017.08.007
55. Lillo-Ródenas, M.A., Ros, A., Fuente, E., Montes-Morán, M.A., Martin, M.J., Linares-Solano, A.: Further insights into the activation process of sewage sludge-based precursors by alkaline hydroxides. Chem. Eng. J. 142, 168–174 (2008). doi:10.1016/j.cej.2007.11.021
56. Zhang, B., Xiong, S., Xiao, B., Yu, D., Jia, X.: Mechanism of wet sewage sludge pyrolysis in a tubular furnace. Int. J. Hydrog. Energy. 36, 355–363 (2011). doi:10.1016/j.ijhydene.2010.05.100
57. Fullana, A., Conesa, J.A., Font, R., Martín-Gullón, I.: Pyrolysis of sewage sludge: nitrogenated compounds and pretreatment effects. J. Anal. Appl. Pyrolysis. 68–69, 561–575 (2003). doi:10.1016/S0165-2370(03)00052-4
58. Hagemann, N., Spokas, K., Schmidt, H.-P., Kägi, R., Böhler, M., Bucheli, T.: Activated carbon, biochar and charcoal: linkages and synergies across pyrogenic carbon's ABCs. Water. 10, 182 (2018). doi:10.3390/w10020182
59. Iriarte-Velasco, U., Ayastuy, J.L., Zudaire, L., Sierra, I.: An insight into the reactions occurring during the chemical activation of bone char. Chem. Eng. J. 251, 217–227 (2014). doi:10.1016/j.cej.2014.04.048
60. Lehmann, J., Joseph, S. eds: Biochar for Environmental Management: Science, Technology and Implementation. Routledge, Abingdon, UK (2015)
61. Jindo, K., Mizumoto, H., Sawada, Y., Sanchez-Monedero, M.A., Sonoki, T.: Physical and chemical characterization of biochars derived from different agricultural residues. Biogeosciences. 11, 6613–6621 (2014). doi:10.5194/bg-11-6613-2014
62. Hung, C.-Y., Tsai, W.-T., Chen, J.-W., Lin, Y.-Q., Chang, Y.-M.: Characterization of biochar prepared from biogas digestate. Waste Manag. 66, 53–60 (2017). doi:10.1016/j.wasman.2017.04.034
63. Vu, K.A., Tawfiq, K., Chen, G.: Rhamnolipid transport in biochar-amended agricultural soil. Water. Air. Soil Pollut. 226, 256 (2015). doi:10.1007/s11270-015-2497-0
64. Chen, B., Chen, Z.: Sorption of naphthalene and 1-naphthol by biochars of orange peels with different pyrolytic temperatures. Chemosphere. 76, 127–133 (2009). doi:10.1016/j.chemosphere.2009.02.004

65. Graber, E.R., Tsechansky, L., Gerstl, Z., Lew, B.: High surface area biochar negatively impacts herbicide efficacy. Plant Soil. 353, 95–106 (2012). doi:10.1007/s11104-011-1012-7
66. Gray, M., Johnson, M.G., Dragila, M.I., Kleber, M.: Water uptake in biochars: the roles of porosity and hydrophobicity. Biomass Bioenergy. 61, 196–205 (2014). doi:10.1016/j.biombioe.2013.12.010
67. Rehrah, D., Reddy, M.R., Novak, J.M., Bansode, R.R., Schimmel, K.A., Yu, J., Watts, D.W., Ahmedna, M.: Production and characterization of biochars from agricultural by-products for use in soil quality enhancement. J. Anal. Appl. Pyrolysis. 108, 301–309 (2014). doi:10.1016/j.jaap.2014.03.008
68. Liu, Z., Zhang, F.-S., Wu, J.: Characterization and application of chars produced from pinewood pyrolysis and hydrothermal treatment. Fuel. 89, 510–514 (2010). doi:10.1016/j.fuel.2009.08.042
69. Asmadi, M., Kawamoto, H., Saka, S.: Pyrolysis reactions of Japanese cedar and Japanese beech woods in a closed ampoule reactor. J. Wood Sci. 56, 319–330 (2010). doi:10.1007/s10086-009-1097-2
70. Asmadi, M., Kawamoto, H., Saka, S.: Gas- and solid/liquid-phase reactions during pyrolysis of softwood and hardwood lignins. J. Anal. Appl. Pyrolysis. 92, 417–425 (2011). doi:10.1016/j.jaap.2011.08.003
71. Anca-Couce, A., Obernberger, I.: Application of a detailed biomass pyrolysis kinetic scheme to hardwood and softwood torrefaction. Fuel. 167, 158–167 (2016). doi:10.1016/j.fuel.2015.11.062
72. McKendry, P.: Energy production from biomass (part 1): overview of biomass. Rev. Issue. 83, 37–46 (2002). doi:10.1016/S0960-8524(01)00118-3
73. Ding, Y., Ezekoye, O.A., Lu, S., Wang, C., Zhou, R.: Comparative pyrolysis behaviors and reaction mechanisms of hardwood and softwood. Energy Convers. Manag. 132, 102–109 (2017). doi:10.1016/j.enconman.2016.11.016
74. Bourke, J., Manley-Harris, M., Fushimi, C., Dowaki, K., Nunoura, T., Antal, M.J.: Do all carbonized charcoals have the same chemical structure? 2. A model of the chemical structure of carbonized charcoal. Ind. Eng. Chem. Res. 46, 5954–5967 (2007). doi:10.1021/ie070415u
75. Guo, J., Chen, B.: Insights on the molecular mechanism for the recalcitrance of biochars: interactive effects of carbon and silicon components. Environ. Sci. Technol. 48, 9103–9112 (2014). doi:10.1021/es405647e
76. Zhao, L., Cao, X., Mašek, O., Zimmerman, A.: Heterogeneity of biochar properties as a function of feedstock sources and production temperatures. J. Hazard. Mater. 256–257, 1–9 (2013). doi:10.1016/j.jhazmat.2013.04.015
77. Figueiredo, J.L., Pereira, M.F.R., Freitas, M.M.A., Órfão, J.J.M.: Modification of the surface chemistry of activated carbons. Carbon. 37, 1379–1389 (1999). doi:10.1016/S0008-6223(98)00333-9
78. Frackowiak, E., Béguin, F.: Carbon materials for the electrochemical storage of energy in capacitors. Carbon. 39, 937–950 (2001). doi:10.1016/S0008-6223(00)00183-4
79. Li, Y., Shao, J., Wang, X., Deng, Y., Yang, H., Chen, H.: Characterization of modified biochars derived from bamboo pyrolysis and their utilization for target component (furfural) adsorption. Energy Fuels. 28, 5119–5127 (2014). doi:10.1021/ef500725c

80. Braghiroli, F.L., Fierro, V., Izquierdo, M.T., Parmentier, J., Pizzi, A., Celzard, A.: Nitrogen-doped carbon materials produced from hydrothermally treated tannin. Carbon. 50, 5411–5420 (2012). doi:10.1016/j.carbon.2012.07.027
81. Braghiroli, F.L., Fierro, V., Szczurek, A., Stein, N., Parmentier, J., Celzard, A.: Hydrothermally treated aminated tannin as precursor of N-doped carbon gels for supercapacitors. Carbon. 90, 63–74 (2015). doi:10.1016/j.carbon.2015.03.038
82. Ma, Y., Liu, W.-J., Zhang, N., Li, Y.-S., Jiang, H., Sheng, G.-P.: Polyethylenimine modified biochar adsorbent for hexavalent chromium removal from the aqueous solution. Bioresour. Technol. 169, 403–408 (2014). doi:10.1016/j.biortech.2014.07.014
83. Dehkhoda, A.M., Ellis, N.: Biochar-based catalyst for simultaneous reactions of esterification and transesterification. Catal. Process. Clean Energy Waste Minimization Green Chem. 207, 86–92 (2013). doi:10.1016/j.cattod.2012.05.034
84. Dehkhoda, A.M., West, A.H., Ellis, N.: Biochar based solid acid catalyst for biodiesel production. Appl. Catal. Gen. 382, 197–204 (2010). doi:10.1016/j.apcata.2010.04.051
85. Gil, R.R., Ruiz, B., Lozano, M.S., Fuente, E.: Influence of the pyrolysis step and the tanning process on KOH-activated carbons from biocollagenic wastes. Prospects as adsorbent for CO_2 capture. J. Anal. Appl. Pyrolysis. 110, 194–204 (2014). doi:10.1016/j.jaap.2014.09.001
86. Titirici, M.-M. ed: Sustainable Carbon Materials from Hydrothermal Processes. Wiley, Chichester, UK (2013)
87. Liu, W.-J., Jiang, H., Yu, H.-Q.: Development of biochar-based functional materials: toward a sustainable platform carbon material. Chem. Rev. 115, 12251–12285 (2015). doi:10.1021/acs.chemrev.5b00195
88. Shen, Y., Yoshikawa, K.: Tar conversion and vapor upgrading via in situ catalysis using silica-based nickel nanoparticles embedded in rice husk char for biomass pyrolysis/gasification. Ind. Eng. Chem. Res. 53, 10929–10942 (2014). doi:10.1021/ie501843y
89. Liu, W.-J., Tian, K., Jiang, H., Yu, H.-Q.: Harvest of Cu NP anchored magnetic carbon materials from Fe/Cu preloaded biomass: their pyrolysis, characterization, and catalytic activity on aqueous reduction of 4-nitrophenol. Green Chem. 16, 4198 (2014). doi:10.1039/C4GC00599F
90. Richardson, Y., Blin, J., Volle, G., Motuzas, J., Julbe, A.: In situ generation of Ni metal nanoparticles as catalyst for H_2-rich syngas production from biomass gasification. Appl. Catal. Gen. 382, 220–230 (2010). doi:10.1016/j.apcata.2010.04.047
91. Richardson, Y., Motuzas, J., Julbe, A., Volle, G., Blin, J.: Catalytic investigation of in situ generated Ni metal nanoparticles for tar conversion during biomass pyrolysis. J. Phys. Chem. C. 117, 23812–23831 (2013). doi:10.1021/jp408191p
92. Hua, M., Zhang, S., Pan, B., Zhang, W., Lv, L., Zhang, Q.: Heavy metal removal from water/wastewater by nanosized metal oxides: a review. Nanotechnologies Treat. Water Air Soil. 211, 317–331 (2012). doi:10.1016/j.jhazmat.2011.10.016
93. Yao, Y., Gao, B., Chen, J., Zhang, M., Inyang, M., Li, Y., Alva, A., Yang, L.: Engineered carbon (biochar) prepared by direct pyrolysis of Mg-accumulated tomato tissues: characterization and phosphate removal potential. Bioresour. Technol. 138, 8–13 (2013). doi:10.1016/j.biortech.2013.03.057
94. Zhang, M., Gao, B., Yao, Y., Xue, Y., Inyang, M.: Synthesis of porous MgO-biochar nanocomposites for removal of phosphate and nitrate from aqueous solutions. Chem. Eng. J. 210, 26–32 (2012). doi:10.1016/j.cej.2012.08.052

95. Barth, J.V., Costantini, G., Kern, K.: Engineering atomic and molecular nanostructures at surfaces. Nature. 437, 671–679 (2005). doi:10.1038/nature04166
96. Braghiroli, F.L., Fierro, V., Szczurek, A., Gadonneix, P., Ghanbaja, J., Parmentier, J., Medjahdi, G., Celzard, A.: Hydrothermal treatment of tannin: a route to porous metal oxides and metal/carbon hybrid materials. Inorganics. 5, 7 (2017). doi:10.3390/inorganics5010007
97. Fan, Z., Huang, X., Tan, C., Zhang, H.: Thin metal nanostructures: synthesis, properties and applications. Chem Sci. 6, 95–111 (2015). doi:10.1039/C4SC02571G
98. Zhu, C., Du, D., Eychmüller, A., Lin, Y.: Engineering ordered and nonordered porous noble metal nanostructures: synthesis, assembly, and their applications in electrochemistry. Chem. Rev. 115, 8896–8943 (2015). doi:10.1021/acs.chemrev.5b00255
99. Bose, P., Aparna Bose, M., Kumar, S.: Critical evaluation of treatment strategies involving adsorption and chelation for wastewater containing copper, zinc and cyanide. Adv. Environ. Res. 7, 179–195 (2002). doi:10.1016/S1093-0191(01)00125-3
100. Sharma, R., Sarswat, A., Pittman, C.U., Mohan, D.: Cadmium and lead remediation using magnetic and non-magnetic sustainable biosorbents derived from *Bauhinia purpurea* pods. RSC Adv. 7, 8606–8624 (2017). doi:10.1039/C6RA25295H
101. Nartey, O.D., Zhao, B.: Biochar preparation, characterization, and adsorptive capacity and Its effect on bioavailability of contaminants: an overview. Adv. Mater. Sci. Eng. 2014, 1–12 (2014). doi:10.1155/2014/715398
102. Renu, Agarwal, M., Singh, K.: Heavy metal removal from wastewater using various adsorbents: a review. J. Water Reuse Desalination. 7, 387–419 (2017). doi:10.2166/wrd.2016.104
103. Bhatnagar, A., Hogland, W., Marques, M., Sillanpää, M.: An overview of the modification methods of activated carbon for its water treatment applications. Chem. Eng. J. 219, 499–511 (2013). doi:10.1016/j.cej.2012.12.038
104. Chang, Q., Lin, W., Ying, W.: Preparation of iron-impregnated granular activated carbon for arsenic removal from drinking water. J. Hazard. Mater. 184, 515–522 (2010). doi:10.1016/j.jhazmat.2010.08.066
105. Cheremisinoff, N.P.: Handbook of water and wastewater treatment technologies. Butterworth-Heinemann, Oxford, UK (2001)
106. Dias, J.M., Alvim-Ferraz, M.C.M., Almeida, M.F., Rivera-Utrilla, J., Sánchez-Polo, M.: Waste materials for activated carbon preparation and its use in aqueous-phase treatment: A review. J. Environ. Manage. 85, 833–846 (2007). doi:10.1016/j.jenvman.2007.07.031
107. Rodríguez-Reinoso, F., Linares-Solano, A.: Microporous structure of activated carbons as revealed by adsorption methods. In: Thrower, P.A. (ed.) Chemistry and Physics of Carbon. pp. 1–146. Marcel Dekker Inc., New York (1989)
108. Knobloch, J.O., Malo, R.V.: Removal of metal contaminants from activated carbon, US3168485A (1965)
109. Kosaka, H., Hirota, H., Iwashima, Y.: Chemically activated shaped carbon, process for producing same and use thereof, US 5039651 A (1991)
110. Armstrong, D.W., Flanigan, V.J., James, W.J., Li, J., Rundlett, K.L.: Activated carbon produced from agricultural residues, US5883040A (1999)
111. Bento, L.R.S.M., Rein, P.W.: Chemical regeneration of activated carbon, US20080286193A1 (2008)
112. Hong, J., White, C.A., Wallace, D., Lavelle, P., Scribner, D.: Method for production of activated carbon, US9682363B2 (2017)

113. Lima, I.M., Marshall, W.E.: Activated carbons from animal manure, US7524795B1 (2009)
114. Gao, B., Inyang, M., Yao, Y., Pullammanappallil, P.: Biologically activated biochar, methods of making biologically activated biochar, and methods of removing contaminants from water, WO2011097183A2 (2011)
115. Rodríguez-Reinoso, F., Molina-Sabio, M.: Activated carbons from lignocellulosic materials by chemical and/or physical activation: an overview. Carbon. 30, 1111–1118 (1992). doi:10.1016/0008-6223(92)90143-K
116. Calo, J.M., Perkins, M.T.: A heterogeneous surface model for the "steady-state" kinetics of the boudouard reaction. Carbon. 25, 395–407 (1987). doi:10.1016/0008-6223(87)90011-X
117. Rodríguez-Reinoso, F., Molina-Sabio, M.: Textural and chemical characterization of microporous carbons. Adv. Colloid Interface Sci. 76–77, 271–294 (1998). doi:10.1016/S0001-8686(98)00049-9
118. Rodríguez-Reinoso, F.: Production and Applications of Activated Carbons. In: Schüth, F., Sing, K.S.W., and Weitkamp, J. (eds.) Handbook of Porous Solids. pp. 1766–1827. Wiley-VCH Verlag GmbH, Weinheim, Germany (2002)
119. Marsh, H. ed: Activated Carbon Compendium: A Collection of Papers from the Journal Carbon 1996-2000. Gulf Professional Publishing, North Shields, UK (2001)
120. Guo, J., Lua, A.C.: Characterization of adsorbent prepared from oil-palm shell by CO_2 activation for removal of gaseous pollutants. Mater. Lett. 55, 334–339 (2002). doi:10.1016/S0167-577X(02)00388-9
121. Hamza, U.D., Nasri, N.S., Amin, N.S., Mohammed, J., Zain, H.M.: Characteristics of oil palm shell biochar and activated carbon prepared at different carbonization times. Desalination Water Treat. 57, 7999–8006 (2016). doi:10.1080/19443994.2015.1042068
122. Chang, C.-F., Chang, C.-Y., Tsai, W.-T.: Effects of burn-off and activation temperature on preparation of activated carbon from corn cob agrowaste by CO_2 and steam. J. Colloid Interface Sci. 232, 45–49 (2000). doi:10.1006/jcis.2000.7171
123. Ngernyen, Y., Tangsathitkulchai, C., Tangsathitkulchai, M.: Porous properties of activated carbon produced from eucalyptus and wattle wood by carbon dioxide activation. Korean J. Chem. Eng. 23, 1046–1054 (2006). doi:10.1007/s11814-006-0028-9
124. Grima-Olmedo, C., Ramírez-Gómez, Á., Gómez-Limón, D., Clemente-Jul, C.: Activated carbon from flash pyrolysis of eucalyptus residue. Heliyon. 2, 1–18 (2016). doi:10.1016/j.heliyon.2016.e00155
125. Işıtan, S., Ceylan, S., Topcu, Y., Hintz, C., Tefft, J., Chellappa, T., Guo, J., Goldfarb, J.L.: Product quality optimization in an integrated biorefinery: conversion of pistachio nutshell biomass to biofuels and activated biochars via pyrolysis. Energy Convers. Manag. 127, 576–588 (2016). doi:10.1016/j.enconman.2016.09.031
126. Jung, S.-H., Kim, J.-S.: Production of biochars by intermediate pyrolysis and activated carbons from oak by three activation methods using CO_2. J. Anal. Appl. Pyrolysis. 107, 116–122 (2014). doi:10.1016/j.jaap.2014.02.011
127. Sricharoenchaikul, V., Pechyen, C., Aht-ong, D., Atong, D.: Preparation and characterization of activated carbon from the pyrolysis of physic nut (*Jatropha curcas* L.) waste. Energy Fuels. 22, 31–37 (2008). doi:10.1021/ef700285u
128. Yang, T., Lua, A.C.: Characteristics of activated carbons prepared from pistachio-nut shells by physical activation. J. Colloid Interface Sci. 267, 408–417 (2003). doi:10.1016/S0021-9797(03)00689-1

129. Choi, G.-G., Oh, S.-J., Lee, S.-J., Kim, J.-S.: Production of bio-based phenolic resin and activated carbon from bio-oil and biochar derived from fast pyrolysis of palm kernel shells. Bioresour. Technol. 178, 99–107 (2015). doi:10.1016/j.biortech.2014.08.053
130. Chen, D., Chen, X., Sun, J., Zheng, Z., Fu, K.: Pyrolysis polygeneration of pine nut shell: quality of pyrolysis products and study on the preparation of activated carbon from biochar. Bioresour. Technol. 216, 629–636 (2016). doi:10.1016/j.biortech.2016.05.107
131. Selvaraju, G., Bakar, N.K.A.: Production of a new industrially viable green-activated carbon from *Artocarpus integer* fruit processing waste and evaluation of its chemical, morphological and adsorption properties. J. Clean. Prod. 141, 989–999 (2017). doi:10.1016/j.jclepro.2016.09.056
132. DeGroot, W.F., Richards, G.N.: Relative rates of carbon gasification in oxygen, steam and carbon dioxide. Carbon. 27, 247–252 (1989). doi:10.1016/0008-6223(89)90130-9
133. Rodríguez-Reinoso, F., Molina-Sabio, M., González, M.T.: The use of steam and CO_2 as activating agents in the preparation of activated carbons. Carbon. 33, 15–23 (1995). doi:10.1016/0008-6223(94)00100-E
134. Ryu, S.K., Jin, H., Gondy, D., Pusset, N., Ehrburger, P.: Activation of carbon fibres by steam and carbon dioxide. Carbon. 31, 841–842 (1993). doi:10.1016/0008-6223(93)90025-6
135. Kühl, H., Kashani-Motlagh, M.M., Mühlen, H.-J., van Heek, K.H.: Controlled gasification of different carbon materials and development of pore structure. Fuel. 71, 879–882 (1992). doi:10.1016/0016-2361(92)90236-H
136. Linares-Solano, A., Salinas-Martínez de Lecea, C., Cazorla-Amorós, D., Martín-Gullón, I.: Porosity development during CO_2 and steam activation in a fluidized bed reactor. Energy Fuels. 14, 142–149 (2000). doi:10.1021/ef9900637
137. Wigmans, T.: Industrial aspects of production and use of activated carbons. Proc. Conf. Porosity Carbon Mater. Meas. Appl. 27, 13–22 (1989). doi:10.1016/0008-6223(89)90152-8
138. Molina-Sabio, M., Gonzalez, M.T., Rodriguez-Reinoso, F., Sepúlveda-Escribano, A.: Effect of steam and carbon dioxide activation in the micropore size distribution of activated carbon. Carbon. 34, 505–509 (1996). doi:10.1016/0008-6223(96)00006-1
139. Tomków, K., Siemieniewska, T., Czechowski, F., Jankowska, A.: Formation of porous structures in activated brown-coal chars using O_2, CO_2 and H_2O as activating agents. Fuel. 56, 121–124 (1977). doi:10.1016/0016-2361(77)90129-6
140. Rajapaksha, A.U., Vithanage, M., Ahmad, M., Seo, D.-C., Cho, J.-S., Lee, S.-E., Lee, S.S., Ok, Y.S.: Enhanced sulfamethazine removal by steam-activated invasive plant-derived biochar. J. Hazard. Mater. 290, 43–50 (2015). doi:10.1016/j.jhazmat.2015.02.046
141. Bouchelta, C., Medjram, M.S., Zoubida, M., Chekkat, F.A., Ramdane, N., Bellat, J.-P.: Effects of pyrolysis conditions on the porous structure development of date pits activated carbon. J. Anal. Appl. Pyrolysis. 94, 215–222 (2012). doi:10.1016/j.jaap.2011.12.014
142. Karaosmanoğlu, F., Işığıgür-Ergüdenler, A., Sever, A.: Biochar from the straw-stalk of rapeseed plant. Energy Fuels. 14, 336–339 (2000). doi:10.1021/ef9901138
143. Ahmad, M., Lee, S.S., Dou, X., Mohan, D., Sung, J.-K., Yang, J.E., Ok, Y.S.: Effects of pyrolysis temperature on soybean stover- and peanut shell-derived biochar properties and TCE adsorption in water. Bioresour. Technol. 118, 536–544 (2012). doi:10.1016/j.biortech.2012.05.042
144. Chun, Y., Sheng, G., Chiou, C.T., Xing, B.: Compositions and sorptive properties of crop residue-derived chars. Environ. Sci. Technol. 38, 4649–4655 (2004). doi:10.1021/es035034w

145. Enders, A., Hanley, K., Whitman, T., Joseph, S., Lehmann, J.: Characterization of biochars to evaluate recalcitrance and agronomic performance. Bioresour. Technol. 114, 644–653 (2012). doi:10.1016/j.biortech.2012.03.022
146. Sun, K., Ro, K., Guo, M., Novak, J., Mashayekhi, H., Xing, B.: Sorption of bisphenol A, 17α-ethinyl estradiol and phenanthrene on thermally and hydrothermally produced biochars. Bioresour. Technol. 102, 5757–5763 (2011). doi:10.1016/j.biortech.2011.03.038
147. Uchimiya, M., Lima, I.M., Klasson, K.T., Wartelle, L.H.: Contaminant immobilization and nutrient release by biochar soil amendment: roles of natural organic matter. Chemosphere. 80, 935–940 (2010). doi:10.1016/j.chemosphere.2010.05.020
148. Baçaoui, A., Yaacoubi, A., Dahbi, A., Bennouna, C., Phan Tan Luu, R., Maldonado-Hodar, F.J., Rivera-Utrilla, J., Moreno-Castilla, C.: Optimization of conditions for the preparation of activated carbons from olive-waste cakes. Carbon. 39, 425–432 (2001). doi:10.1016/S0008-6223(00)00135-4
149. Zhang, Y.-J., Xing, Z.-J., Duan, Z.-K., Meng Li, Wang, Y.: Effects of steam activation on the pore structure and surface chemistry of activated carbon derived from bamboo waste. Appl. Surf. Sci. 315, 279–286 (2014). doi:10.1016/j.apsusc.2014.07.126
150. Lima, I.M., Boykin, D.L., Thomas Klasson, K., Uchimiya, M.: Influence of post-treatment strategies on the properties of activated chars from broiler manure. Chemosphere. 95, 96–104 (2014). doi:10.1016/j.chemosphere.2013.08.027
151. Fan, M., Marshall, W., Daugaard, D., Brown, R.C.: Steam activation of chars produced from oat hulls and corn stover. Bioresour. Technol. 93, 103–107 (2004). doi:10.1016/j.biortech.2003.08.016
152. del Campo, B.: Production of activated carbon from fast pyrolysis biochar and the detoxification of pyrolytic sugars for ethanol fermentation, http://lib.dr.iastate.edu/etd/14691, (2015)
153. Pallarés, J., González-Cencerrado, A., Arauzo, I.: Production and characterization of activated carbon from barley straw by physical activation with carbon dioxide and steam. Biomass Bioenergy. 115, 64–73 (2018). doi:10.1016/j.biombioe.2018.04.015
154. Yahya, M.A., Al-Qodah, Z., Ngah, C.W.Z.: Agricultural bio-waste materials as potential sustainable precursors used for activated carbon production: a review. Renew. Sustain. Energy Rev. 46, 218–235 (2015). doi:10.1016/j.rser.2015.02.051
155. Ozoemena, K.I., Chen, S. eds: Nanomaterials in Advanced Batteries and Supercapacitors. Springer, Switzerland (2016)
156. Armandi, M., Bonelli, B., Geobaldo, F., Garrone, E.: Nanoporous carbon materials obtained by sucrose carbonization in the presence of KOH. Microporous Mesoporous Mater. 132, 414–420 (2010). doi:10.1016/j.micromeso.2010.03.021
157. Ehrburger, P., Addoun, A., Addoun, F., Donnet, J.-B.: Carbonization of coals in the presence of alkaline hydroxides and carbonates: formation of activated carbons. Funcat Cogas 86 Int. Symp. 65, 1447–1449 (1986). doi:10.1016/0016-2361(86)90121-3
158. Lozano-Castelló, D., Calo, J.M., Cazorla-Amorós, D., Linares-Solano, A.: Carbon activation with KOH as explored by temperature programmed techniques, and the effects of hydrogen. Carbon. 45, 2529–2536 (2007). doi:10.1016/j.carbon.2007.08.021
159. Zyzlila Figueroa-Torres, M., Robau-Sánchez, A., De la Torre-Sáenz, L., Aguilar-Elguézabal, A.: Hydrogen adsorption by nanostructured carbons synthesized by chemical activation. Microporous Mesoporous Mater. 98, 89–93 (2007). doi:10.1016/j.micromeso.2006.08.022

160. Li, G., Wang, S., Wu, Q., Wang, F., Shen, B.: Mercury sorption study of halides modified bio-chars derived from cotton straw. Chem. Eng. J. 302, 305–313 (2016). doi:10.1016/j.cej.2016.05.045
161. Jin, H., Wang, X., Gu, Z., Anderson, G., Muthukumarappan, K.: Distillers dried grains with soluble (DDGS) bio-char based activated carbon for supercapacitors with organic electrolyte tetraethylammonium tetrafluoroborate. J. Environ. Chem. Eng. 2, 1404–1409 (2014). doi:10.1016/j.jece.2014.05.019
162. Oh, G.H., Park, C.R.: Preparation and characteristics of rice-straw-based porous carbons with high adsorption capacity. Fuel. 81, 327–336 (2002). doi:10.1016/S0016-2361(01)00171-5
163. Angın, D., Altintig, E., Köse, T.E.: Influence of process parameters on the surface and chemical properties of activated carbon obtained from biochar by chemical activation. Bioresour. Technol. 148, 542–549 (2013). doi:10.1016/j.biortech.2013.08.164
164. Angın, D., Köse, T.E., Selengil, U.: Production and characterization of activated carbon prepared from safflower seed cake biochar and its ability to absorb reactive dyestuff. Appl. Surf. Sci. 280, 705–710 (2013). doi:10.1016/j.apsusc.2013.05.046
165. Mao, H., Zhou, D., Hashisho, Z., Wang, S., Chen, H., Wang, H.H.: Preparation of pinewood- and wheat straw-based activated carbon via a microwave-assisted potassium hydroxide treatment and an analysis of the effects of the microwave activation conditions. BioResources. 10, 809–821 (2014). doi:10.15376/biores.10.1.809-821
166. Zhang, J., Liu, J., Liu, R.: Effects of pyrolysis temperature and heating time on biochar obtained from the pyrolysis of straw and lignosulfonate. Bioresour. Technol. 176, 288–291 (2015). doi:10.1016/j.biortech.2014.11.011
167. Iriarte-Velasco, U., Sierra, I., Zudaire, L., Ayastuy, J.L.: Preparation of a porous biochar from the acid activation of pork bones. Food Bioprod. Process. 98, 341–353 (2016). doi:10.1016/j.fbp.2016.03.003
168. Wu, F.-C., Tseng, R.-L.: Preparation of highly porous carbon from fir wood by KOH etching and CO_2 gasification for adsorption of dyes and phenols from water. J. Colloid Interface Sci. 294, 21–30 (2006). doi:10.1016/j.jcis.2005.06.084
169. Rostamian, R., Heidarpour, M., Mousavi, S.F., Afyuni, M.: Characterization and sodium sorption capacity of biochar and activated carbon prepared from rice husk. J. Agric. Sci. Technol. 17, 1057–1069 (2015)
170. Marcilla, A., García-García, S., Asensio, M., Conesa, J.A.: Influence of thermal treatment regime on the density and reactivity of activated carbons from almond shells. Carbon. 38, 429–440 (2000). doi:10.1016/S0008-6223(99)00123-2
171. Lua, A.C., Yang, T., Guo, J.: Effects of pyrolysis conditions on the properties of activated carbons prepared from pistachio-nut shells. J. Anal. Appl. Pyrolysis. 72, 279–287 (2004). doi:10.1016/j.jaap.2004.08.001
172. Lua, A.C., Lau, F.Y., Guo, J.: Influence of pyrolysis conditions on pore development of oil-palm-shell activated carbons. J. Anal. Appl. Pyrolysis. 76, 96–102 (2006). doi:10.1016/j.jaap.2005.08.001
173. Uchimiya, M., Wartelle, L.H., Lima, I.M., Klasson, K.T.: Sorption of deisopropylatrazine on broiler litter biochars. J. Agric. Food Chem. 58, 12350–12356 (2010). doi:10.1021/jf102152q
174. Braghiroli, F.L., Bouafif, H., Hamza, N., Bouslimi, B., Neculita, C.M., Koubaa, A.: The influence of pilot-scale pyro-gasification and activation conditions on porosity

development in activated biochars. Biomass Bioenergy. 118, 105–114 (2018). doi:10.1016/j.biombioe.2018.08.016

175. Zhang, S., Hu, B., Zhang, L., Xiong, Y.: Effects of torrefaction on yield and quality of pyrolysis char and its application on preparation of activated carbon. J. Anal. Appl. Pyrolysis. 119, 217–223 (2016). doi:10.1016/j.jaap.2016.03.002

176. Park, J., Hung, I., Gan, Z., Rojas, O.J., Lim, K.H., Park, S.: Activated carbon from biochar: influence of its physicochemical properties on the sorption characteristics of phenanthrene. Bioresour. Technol. 149, 383–389 (2013). doi:10.1016/j.biortech.2013.09.085

177. Brewer, C.E., Schmidt-Rohr, K., Satrio, J.A., Brown, R.C.: Characterization of biochar from fast pyrolysis and gasification systems. Environ. Prog. Sustain. Energy. 28, 386–396 (2009). doi:10.1002/ep.10378

178. Azargohar, R., Dalai, A.K.: Biochar as a precursor of activated carbon. Appl. Biochem. Biotechnol. 131, 762–773 (2006). doi:10.1385/ABAB:131:1:762

179. Zhang, T., Walawender, W.P., Fan, L.T., Fan, M., Daugaard, D., Brown, R.C.: Preparation of activated carbon from forest and agricultural residues through CO_2 activation. Chem. Eng. J. 105, 53–59 (2004). doi:10.1016/j.cej.2004.06.011

180. Bhandari, P.N., Kumar, A., Bellmer, D.D., Huhnke, R.L.: Synthesis and evaluation of biochar-derived catalysts for removal of toluene (model tar) from biomass-generated producer gas. Renew. Energy. 66, 346–353 (2014). doi:10.1016/j.renene.2013.12.017

181. Patil, K., Bhoi, P., Huhnke, R., Bellmer, D.: Biomass downdraft gasifier with internal cyclonic combustion chamber: design, construction, and experimental results. Bioresour. Technol. 102, 6286–6290 (2011). doi:10.1016/j.biortech.2011.03.033

182. Sharma, A.M., Kumar, A., Patil, K.N., Huhnke, R.L.: Performance evaluation of a lab-scale fluidized bed gasifier using switchgrass as feedstock. ASABE. 54, 2259–2266 (2011). doi:10.13031/2013.40639

Table captions:

Table 1 Characteristics of thermochemical biomass conversion processes for biochar production: torrefaction; slow, intermediate, fast, and flash pyrolysis; gasification, and hydrothermal carbonization

Figure captions:

Fig. 1 The main products obtained from the thermochemical modification of biomass residue materials and the applications of biochars and activated biochars

Fig. 2 Surface areas of activated biochars as a function of pyro-gasification temperature prepared by: a) CO_2 from pistachio nut shells × (Lua et al. [171]) and ▲ (Işitan et al. [125]), from oil-palm shells ● (Lua et al. [172]) (activated at 1173K), from almond shells ◆ (Marcilla et al. [170]) (activated at 1053K), and from white birch − and black spruce + (Braghiroli et al. [174]) (activated at 973, 1073 and 1173K); and steam from broiler litter × (Uchimiya et al. [173]) (activated at 1073K), and from burcucumber plants + (Rajapaksha et al. [140]) (activated at 573 and 973K); and b) NaOH or KOH from rice straw ◆ (Oh and Park [162]), from debarked loblolly pine chips ● (Park et al. [176]) (activated at 1073K), and from rice husks ▲ (Zhang et al. [175]) (activated at 1098K)

Fig. 3 Surface areas of activated biochars prepared by CO_2 or steam as a function of: a) residence time: made from pistachio nut shells ▲ (Lua et al. [171]), from oil-palm shells ● (Lua et al. [172]) (activated at 1173K) and ◆ (Hamza et al. [121]) (activated at 1073K), and made from date pits ■ (Bouchelta et al. [141]) (activated at 973K); and b) heating rate made with the same materials and conditions as in a)

1395 **Table 1** Characteristics of thermochemical biomass conversion processes for biochar production:
1396 torrefaction; slow, intermediate, fast, and flash pyrolysis; gasification, and hydrothermal
1397 carbonization

	Dry processes						*Wet processes*
	Torrefaction	*Slow pyrolysis*	*Intermediate pyrolysis*	*Fast pyrolysis*	*Flash pyrolysis*	*Gasification*	*Hydrothermal carbonization*
Temperature (K)	473–593	373–1273	~ 773	573–1273	673–1273	> 1073	453−533
Residence Time	~ 10–60 min	5–30 min	10–20 s	< 2 s	< 2 s	10–20 s	5 min−12 h
Heating rate (K min^{-1})	-	5–7	up to 100	300–800	~ 1000	-	5−10
Main product	Torrefied biomass	Biochar	Bio-oil	Bio-oil	Syngas	Syngas	Hydrochar
Solid yield (wt.%)	80	25–35	25	10–20	10–20	10	45−70

1398
1399
1400

1401